Coordination Complexes of NbX_5 (X = F, Cl) with (*N,O*)- and (*O,O*)-Donor Ligands and the First X-Ray Characterization of a Neutral NbF_5 Adduct

Marco Bortoluzzi, Fabio Marchetti, Guido Pampaloni, Margherita Pucino, Stefano Zacchini

Supplementary Material

Figure S1. DFT PBE calculated structure of $NbF_5[\kappa^1(O)\text{-}OC_6H_4CH{=}NHC_6H_3(CHMe_2)_2]$, **2**, with implicit solvation (CH_2Cl_2) and Grimme's correction for dispersion. Selected hydrogen atoms have been omitted for clarity.

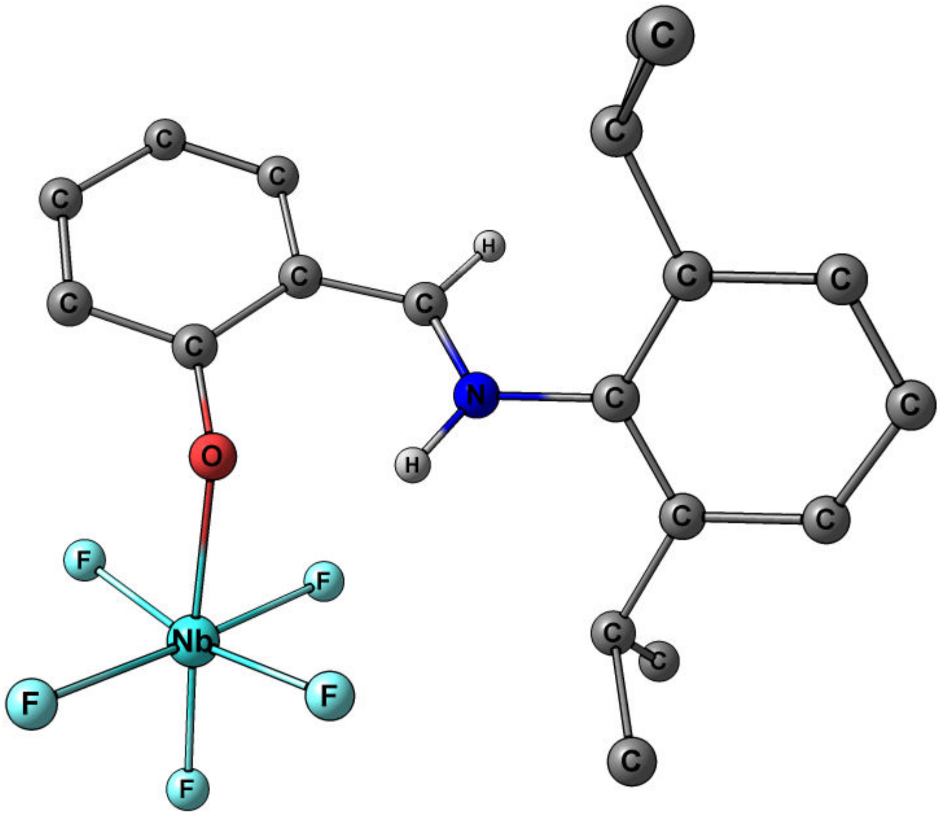

Table S1. Selected computed bond lengths (Å) and angles (°) for **2**.

Bond		**Angle**	
Nb–O	2.006	O–Nb–F (*trans* to O)	176.4
Nb–F (*trans* to O)	1.920	O–Nb–F (*cis* to O)	88.1
Nb–F (*cis* to O)	1.950		87.6
	1.941		83.8
	1.932		81.2
	1.931		
N–H	1.031		
(N)H···F (*shortest*)	2.381		
(N)H···O	2.000		

Figure S2. DFT-calculated possible structures of the product of the reaction of NbF_5 (**1a**) with $saoH_2$, with implicit solvation (CH_2C_{l2}) and Grimme's correction for dispersion. Selected hydrogen atoms have been omitted for clarity.

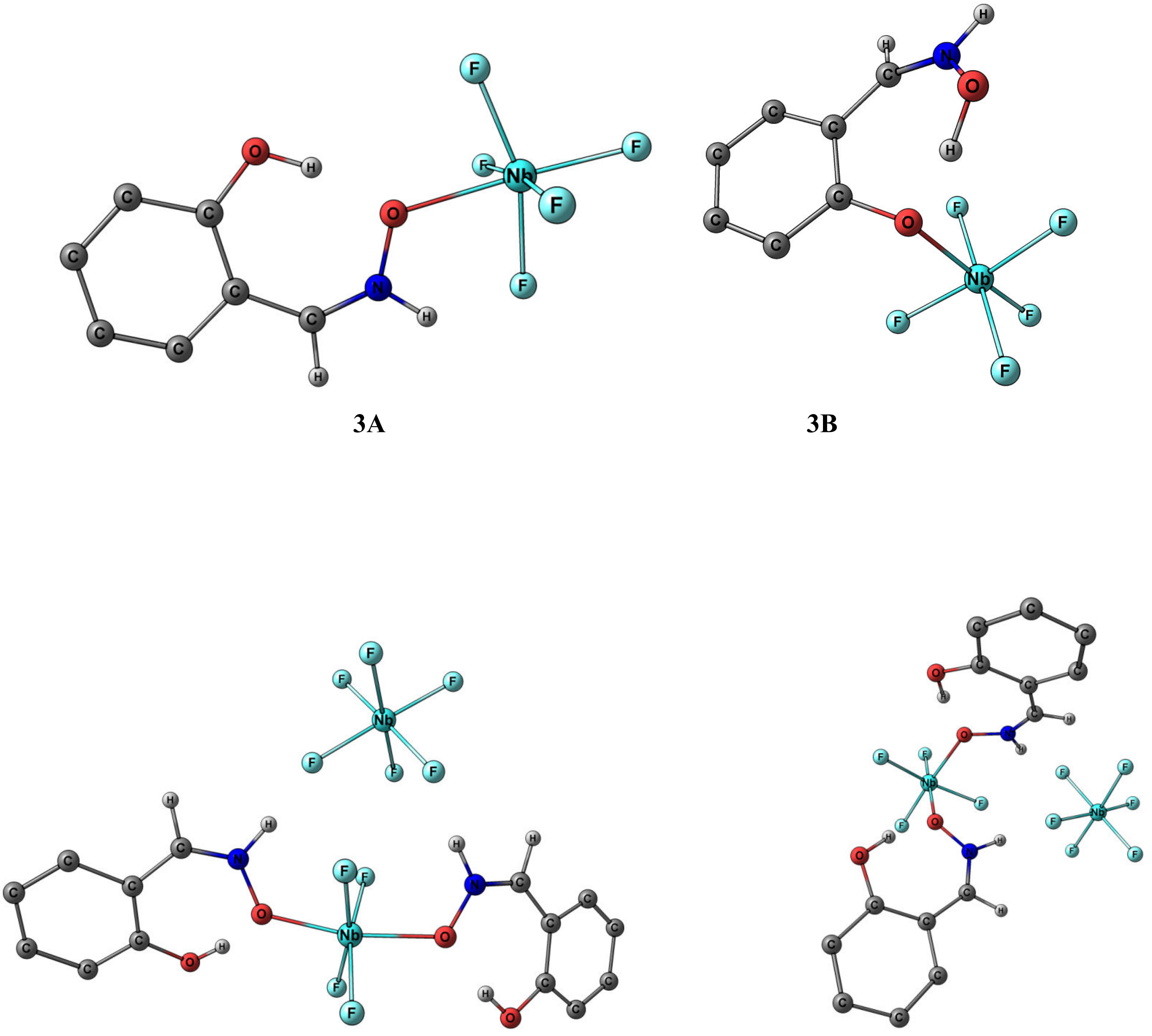

3A **3B**

3C **3D**

Relative energies (Kcal mol^{-1}, referred to Nb unit, corrected for zero-point vibrational energy):

	3A	**3B**	**3C**	**3D**
PBE/COSMO/DNP	–0.9	0	–1.8	–3.9

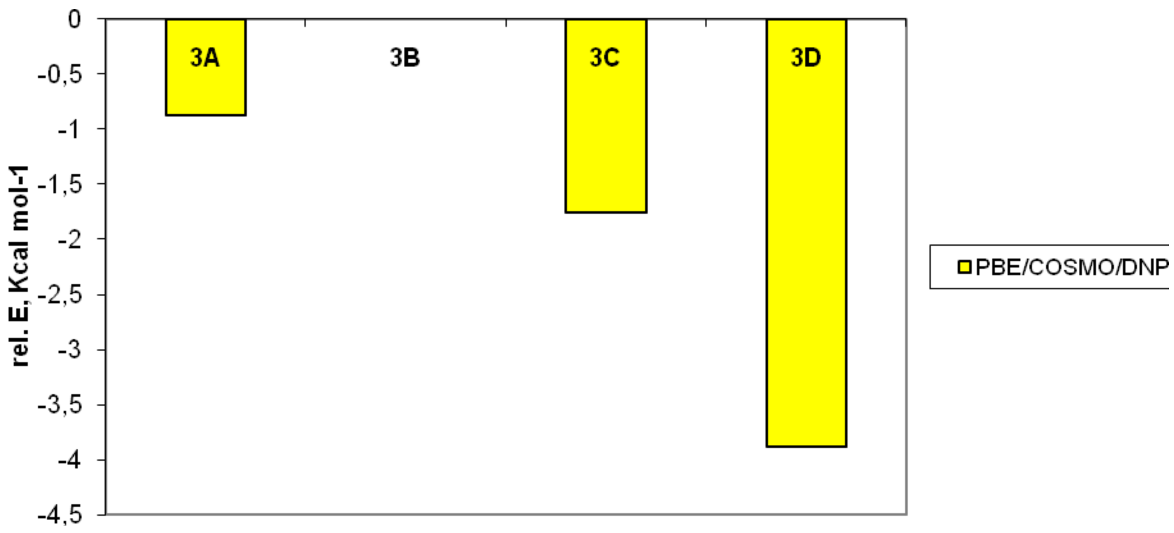

Table S2. Selected computed bond lengths (Å) and angles (°) for **3D**.

Bond		**Angle**	
Nb–O	2.117	O–Nb–O	88.0
	2.084	O–Nb–F (*trans*)	179.4
Nb–F (*trans* to O)	1.910		175.3
	1.903	O–Nb–F (*cis*)	81.4
Nb–F (*cis* to O)	1.917		87.6
	1.903		83.8
Nb–F (NbF_6^-, *average*)	1.939		82.3
N–O	1.351		82.5
	1.351		92.0
O–H	0.998		
	0.997		
(O)H···O	1.648		
	1.634		
N–H	1.039		
	1.035		
(O)H···F (NbF_6^-, *shortest*)	1.818		
	1.732		

Figure S3-a. DFT PBE calculated possible structures of product of the reaction of $NbCl_5$, **1b**, with dpimpH, with implicit solvation (CH_2Cl_2) and Grimme's correction for dispersion. Selected hydrogen atoms have been omitted for clarity.

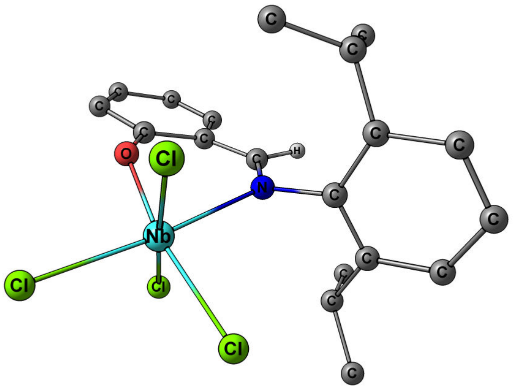

4aA

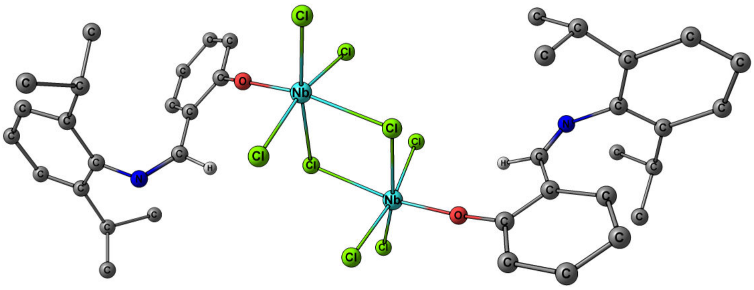

4aB

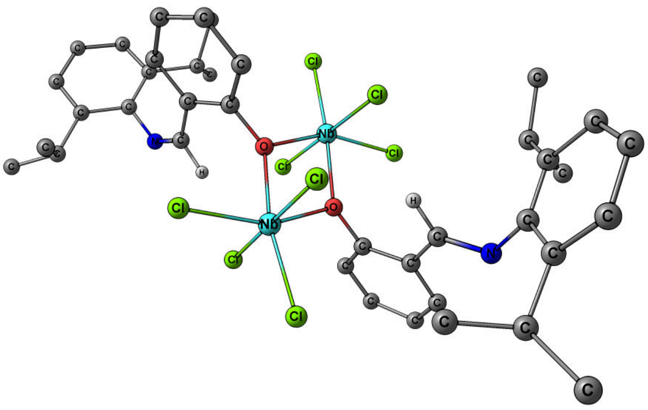

4aC

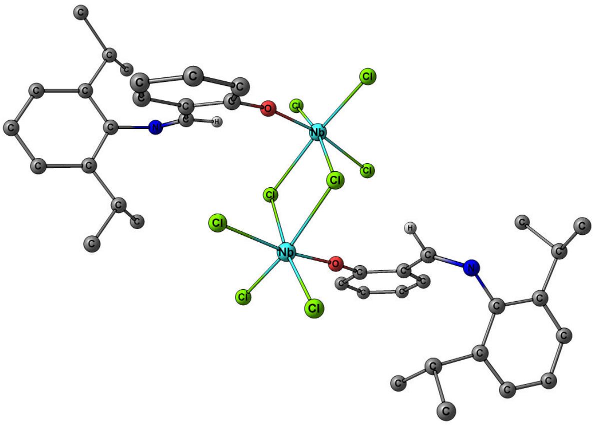

4aD

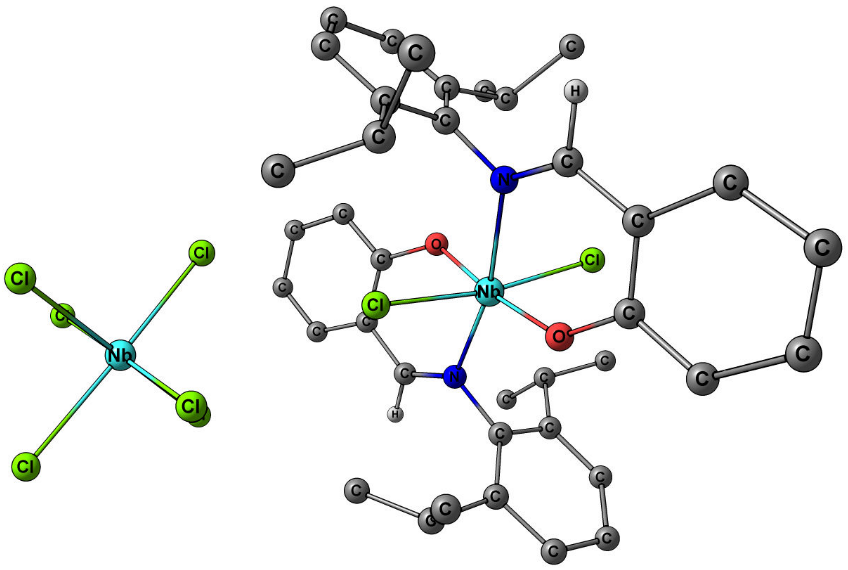

4aE

Relative energies (Kcal mol^{-1}, corrected for zero-point vibrational energy, referred to $NbCl_5L$ formula):

	4aA	**4aB**	**4aC**	**4aD**	**4aE**
PBE/COSMO/DNP	−13.2	0	−3.0	−5.4	−17.1

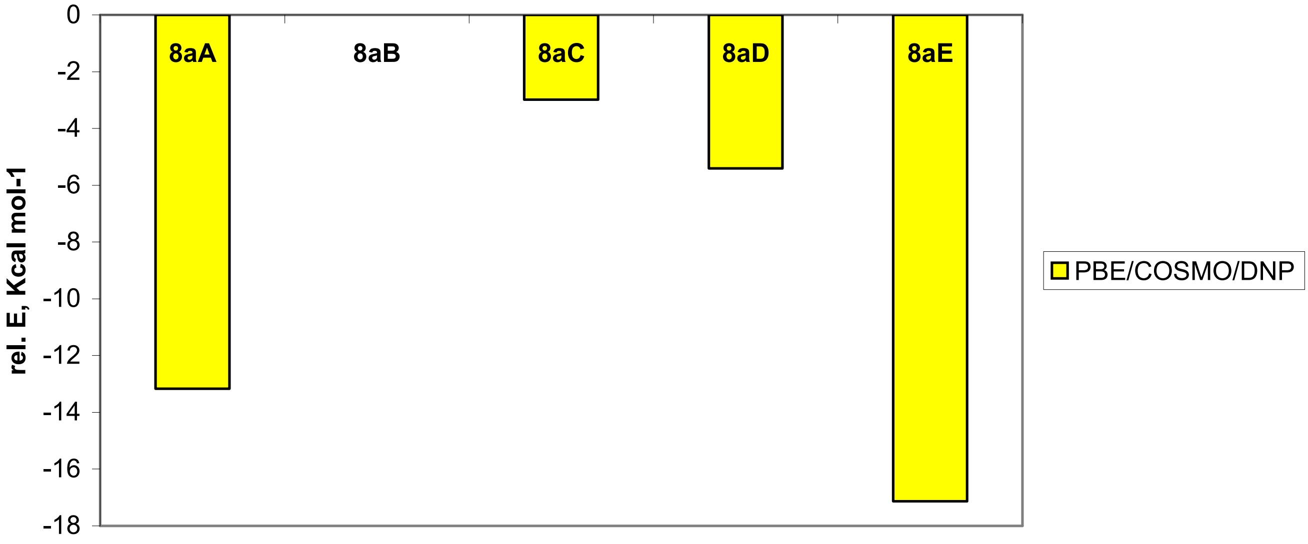

Table S3. Selected computed bond lengths (Å) and angles (°) for **4aE**.

Bond		**Angle**	
Nb–Cl (cation)	2.346	Cl–Nb–Cl (cation)	170.1
	2.393	O–Nb–O	172.9
Nb–O	1.986	N–Nb–N	167.8
	1.942		
Nb–N	2.286		
	2.173		
Nb–Cl (anion, average)	2.397		

Figure S3-b. DFT PBE calculated possible structures of $[NbCl_2(dpimp)_2]^+$, with implicit solvation (CH_2Cl_2) and Grimme's correction for dispersion. Selected hydrogen atoms have been omitted for clarity.

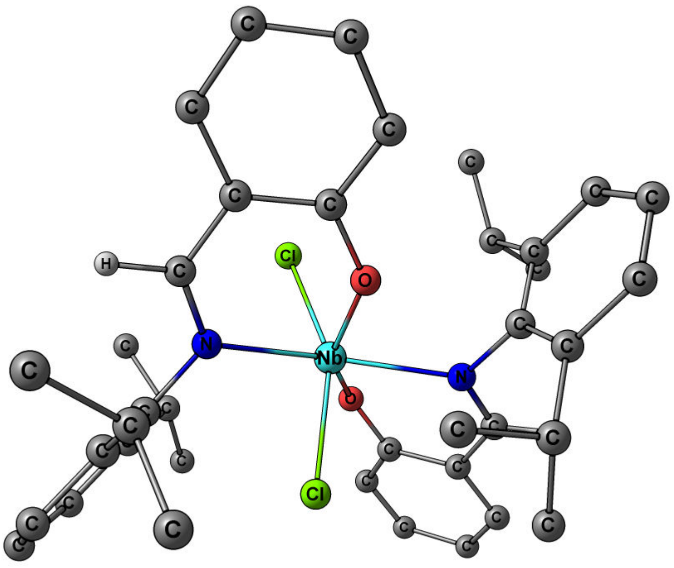

4aE⁺

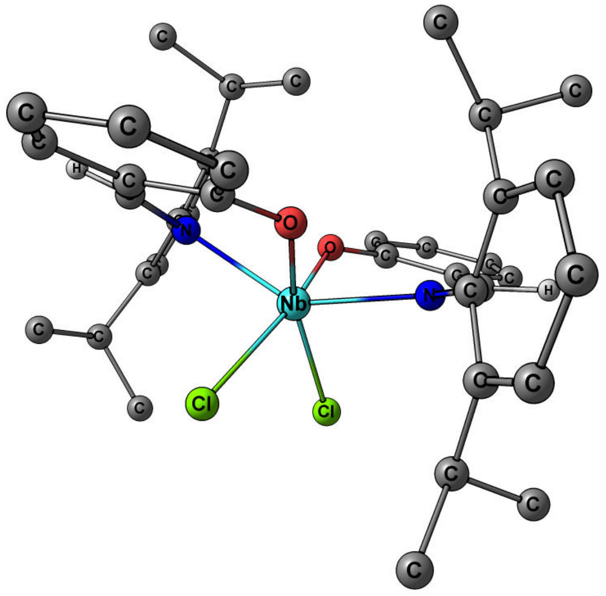

4aF⁺

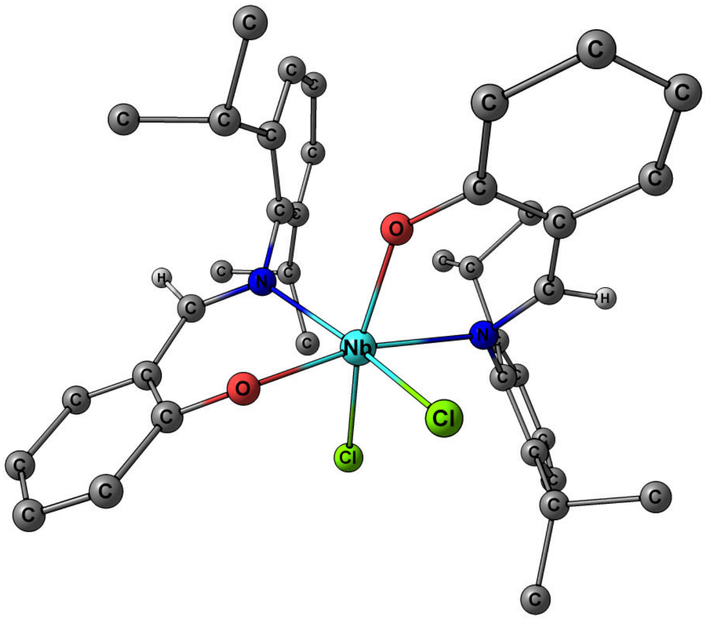

4aG⁺

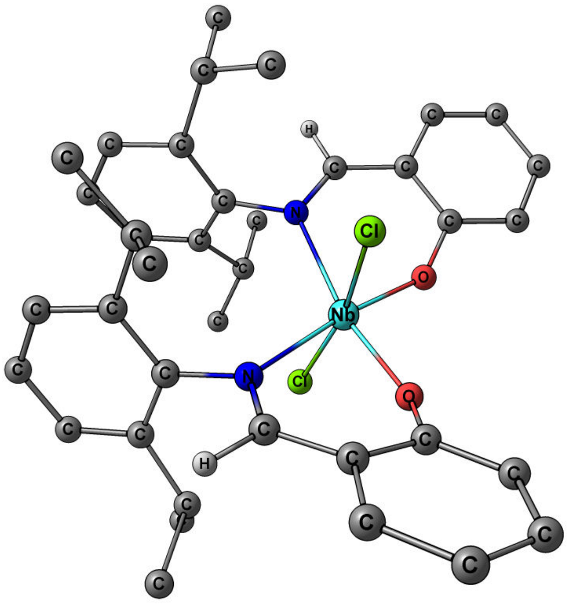

4aH⁺

Relative energies (Kcal mol^{-1}, corrected for zero-point vibrational energy):

	$4aE^+$	**$4aF^+$**	**$4aG^+$**	**$4aH^+$**
PBE/COSMO/DNP	−20.1	−12.7	−9.6	0

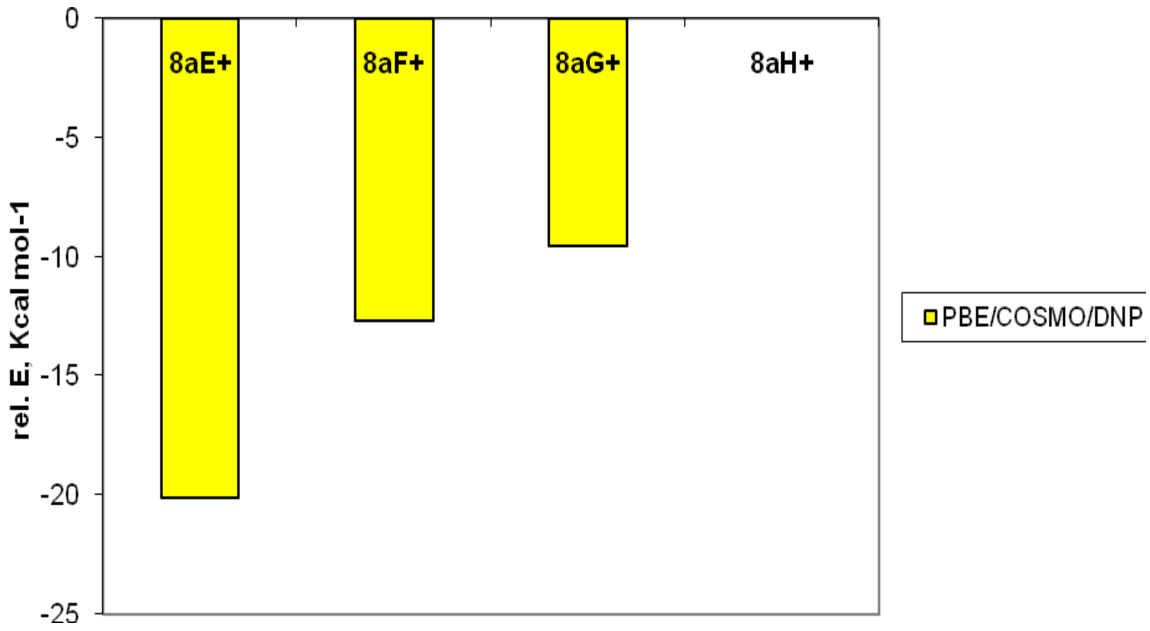
0
-5
-10
-15
-20
-25
rel. E, Kcal mol-1
8aE+
8aF+
8aG+
8aH+
PBE/COSMO/DNP

Figure S4-a. DFT PBE calculated possible structures of $Nb_2Cl_9[\kappa^1(O)\text{-}ON{=}CHC_6H_4OH]$ and $Nb_2Cl_9[\kappa^1(O)\text{-}OC_6H_4CH{=}NOH]$, with implicit solvation (CH_2Cl_2) and Grimme's correction for dispersion. Selected hydrogen atoms have been omitted for clarity.

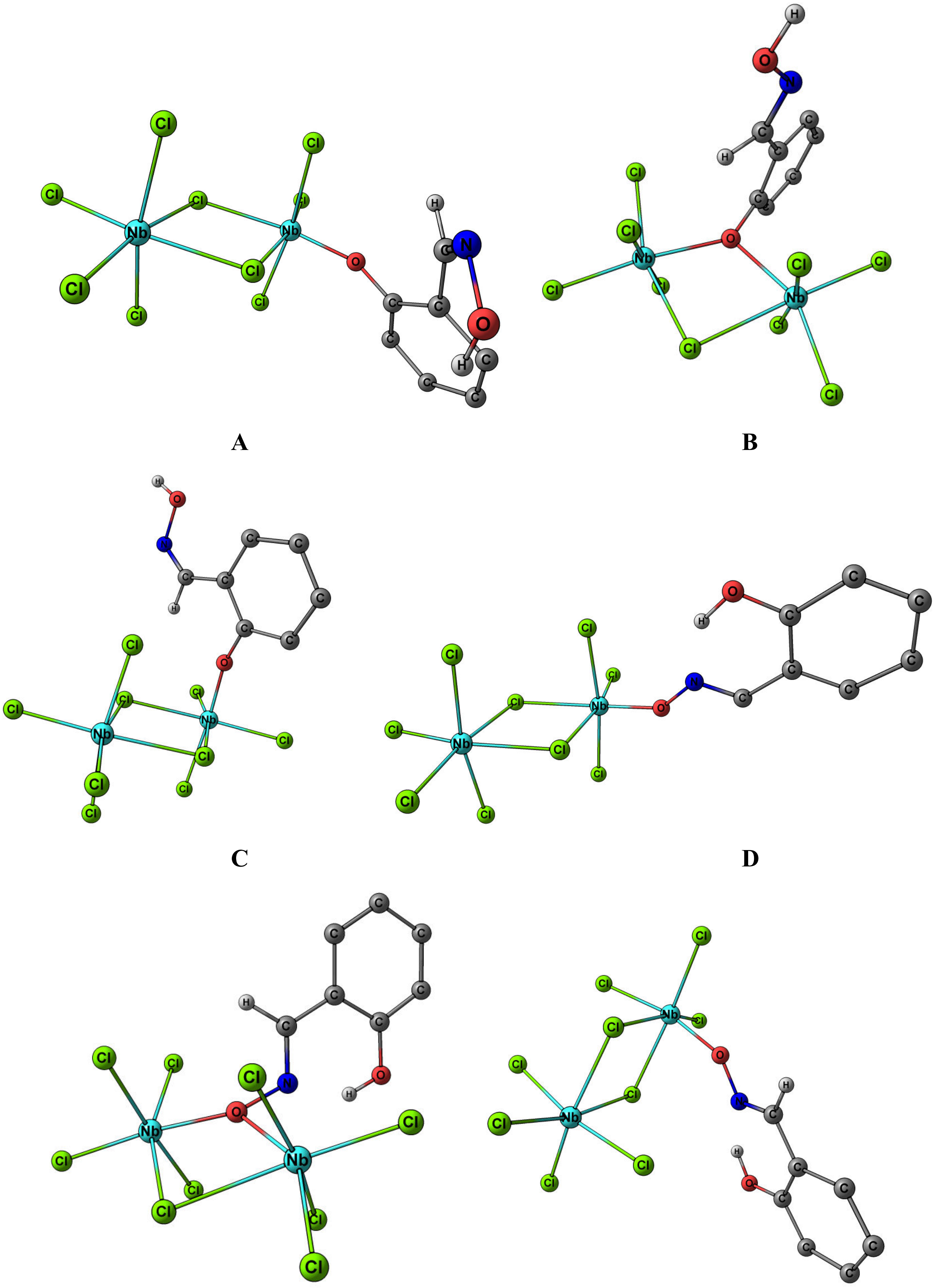

A **B**

C **D**

E **F**

Relative energies (Kcal mol^{-1}, corrected for zero-point vibrational energy)

	A	B	C	D	E	F
PBE/COSMO/DNP	0	–2.8	–4.9	–9.5	–10.4	–9.8

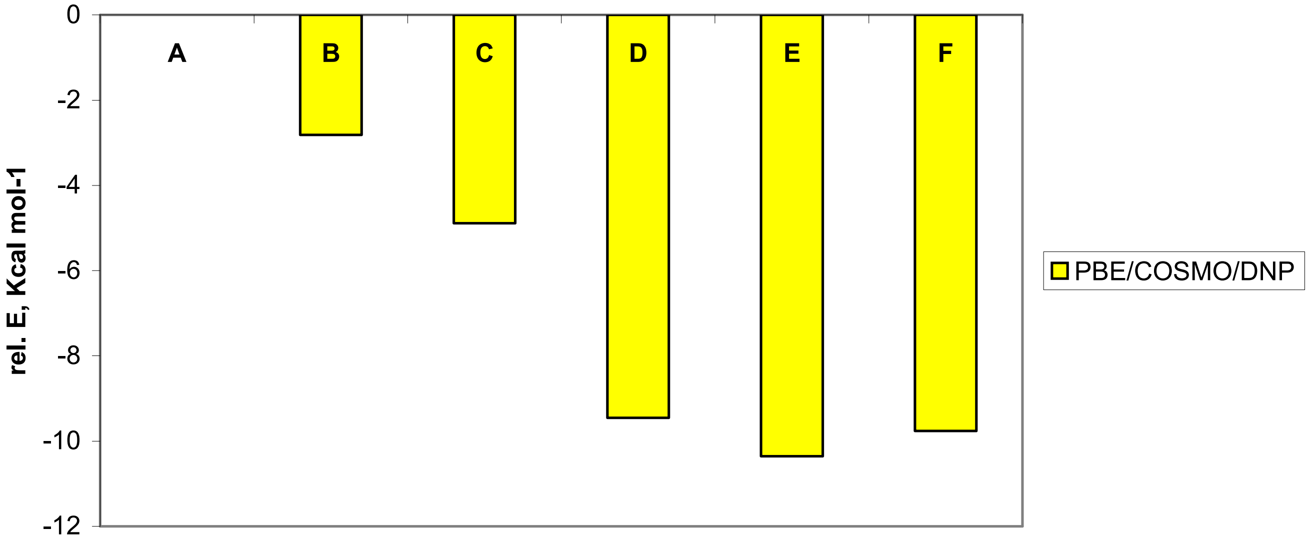

Figure S4-b. DFT PBE calculated possible structures of $Nb_2Cl_8[\kappa^2(O)\text{-}ON{=}CHC_6H_4O]$, with implicit solvation (CH_2Cl_2) and Grimme's correction for dispersion. Selected hydrogen atoms have been omitted for clarity.

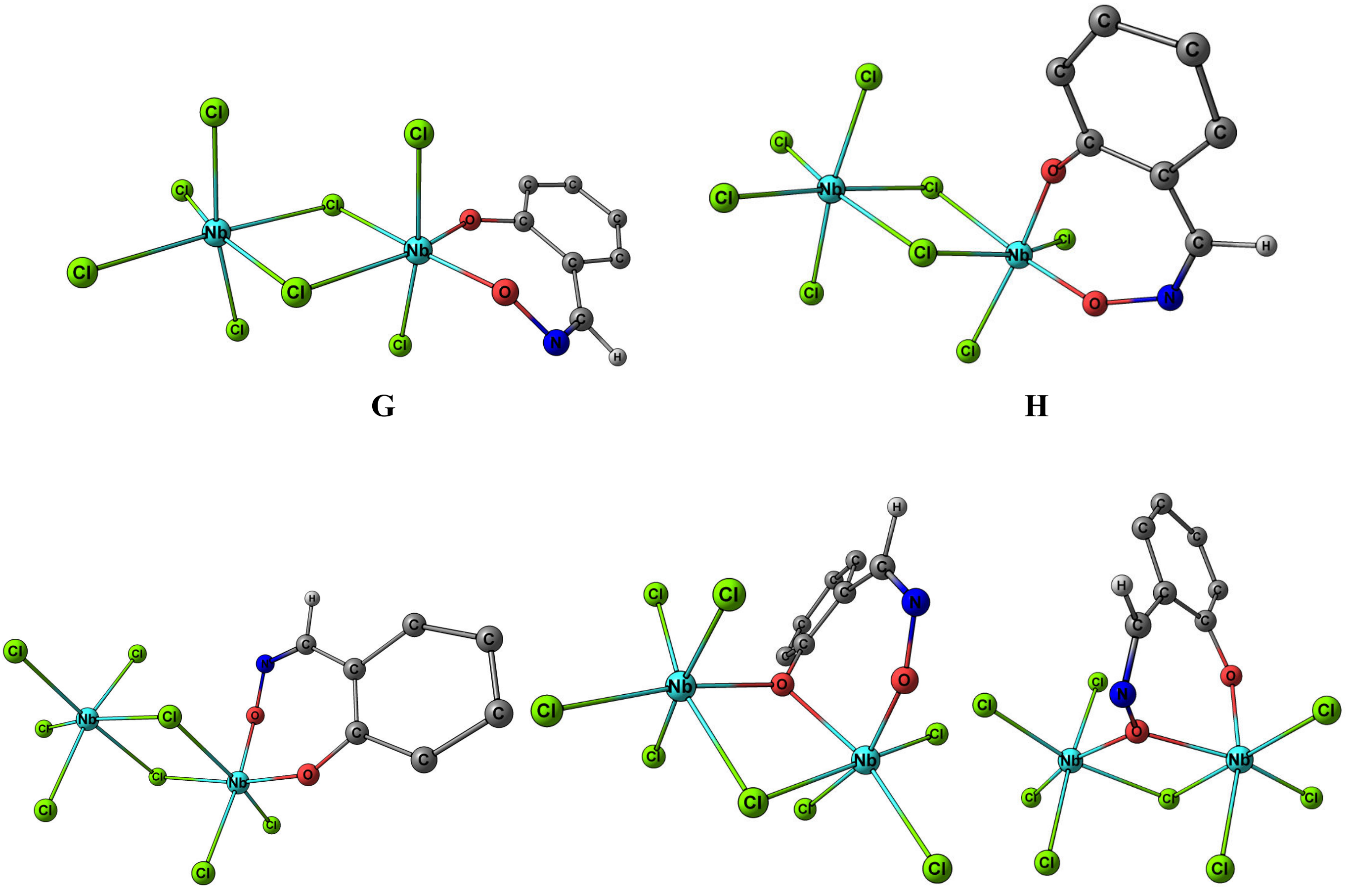

G **H**

I **J** **K**

Relative energies (Kcal mol^{-1}, corrected for zero-point vibrational energy)

	G	H	I	J	K
PBE/COSMO/DNP	0	−1.5	−2.5	−5.9	−7.6

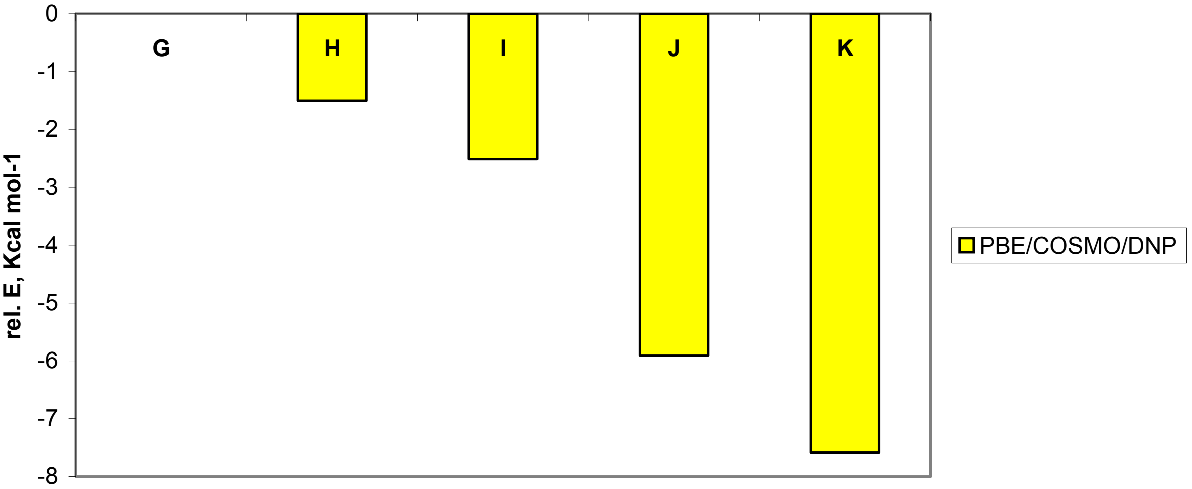

Figure S4-c. DFT PBE calculated possible structures of $Nb_2Cl_7[\kappa^1(O)\text{-saoH}][\kappa^2(O)\text{-sao}]$, **5**, with implicit solvation (CH_2Cl_2) and Grimme's correction for dispersion. Selected hydrogen atoms have been omitted for clarity.

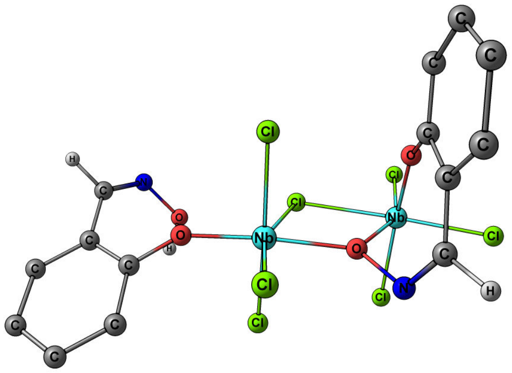

5A

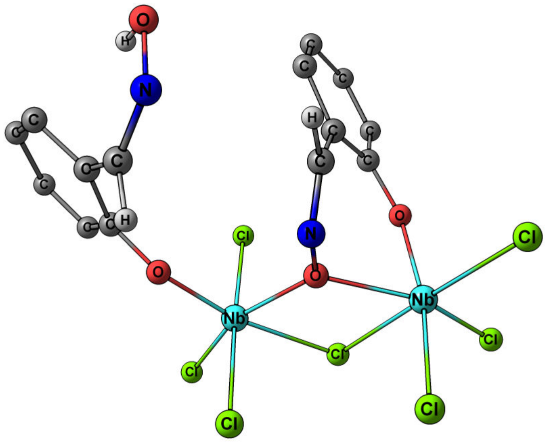

5B

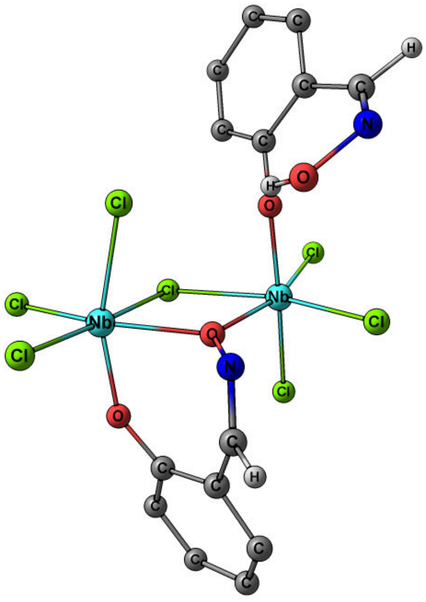

5C

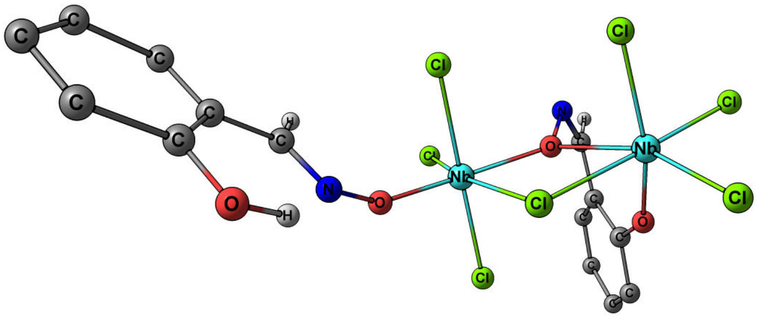

5D

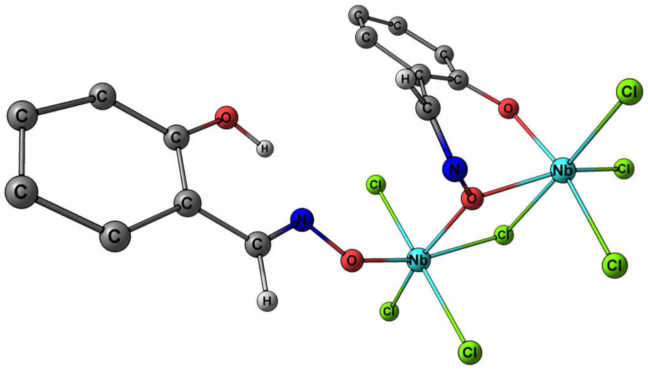

5E

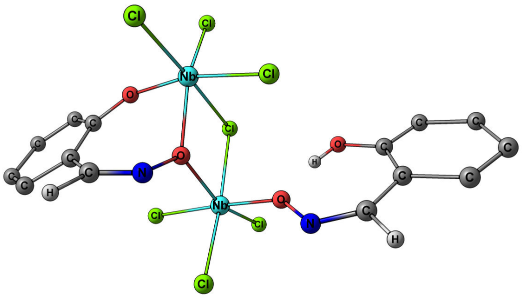

5F

Relative energies (Kcal mol^{-1}, corrected for zero-point vibrational energy)

	5A	5B	5C	5D	5E	5F
PBE/COSMO/DNP	0	–1.7	–0.8	–10.0	–11.5	–1.9

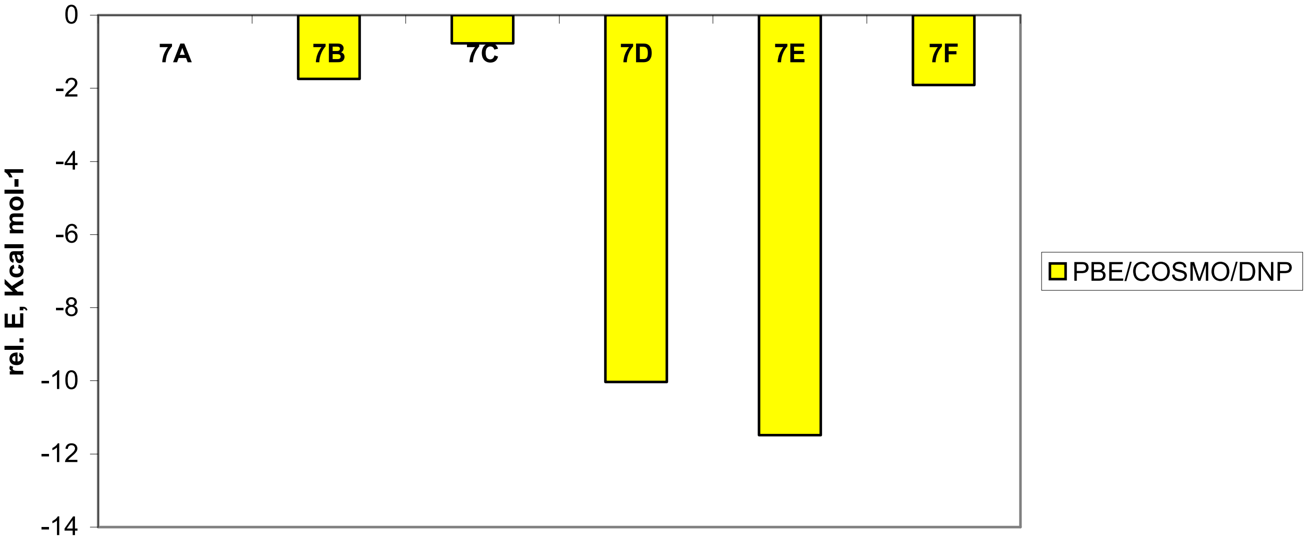

Figure S5. DFT-calculated possible ionic structures of the product of the reaction of NbF_5 (**1a**) with $HO(CH_2)_2NHPh$, with implicit solvation (CH_2Cl_2) and Grimme's correction for dispersion. Selected hydrogen atoms have been omitted for clarity.

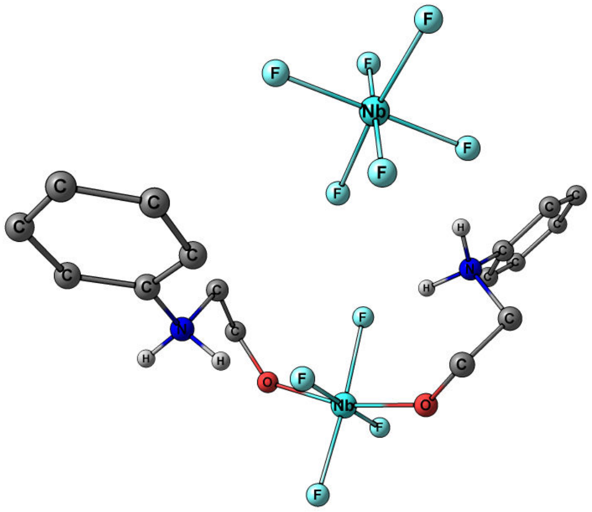

6A

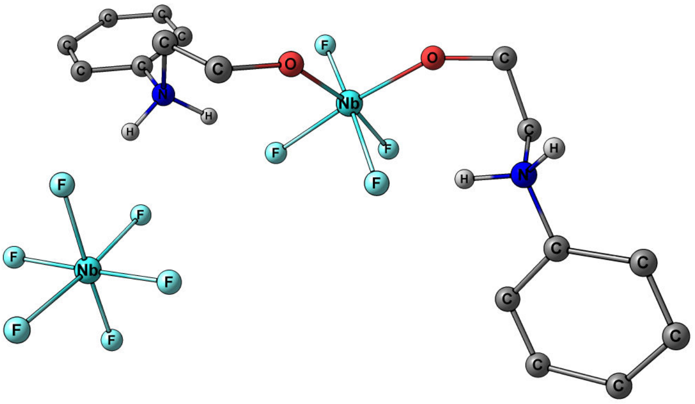

6B

Relative energies (Kcal mol^{-1}, corrected for zero-point vibrational energy, referred to Nb units).

	6A	6B
PBE/COSMO/DNP	−3.1	0

Table S4. Selected computed bond lengths (Å) and angles (°) for the **6A**.

Bond		Angle	
Nb–O	1.936	O–Nb–O	162.5
	1.928	F–Nb–F (cation)	176.7
Nb–F (cation)	2.032		175.9
	2.034		
	1.936		
	1.930		
Nb–F (anion, average)	1.937		
N–H	1.055		
	1.028		
	1.043		
	1.058		

Figure S6. DFT PBE calculated possible structures of the product of the reaction of NbF_5 (**1a**) with bhpfH, with implicit solvation (CH_2Cl_2) and Grimme's correction for dispersion. Selected hydrogen atoms have been omitted for clarity.

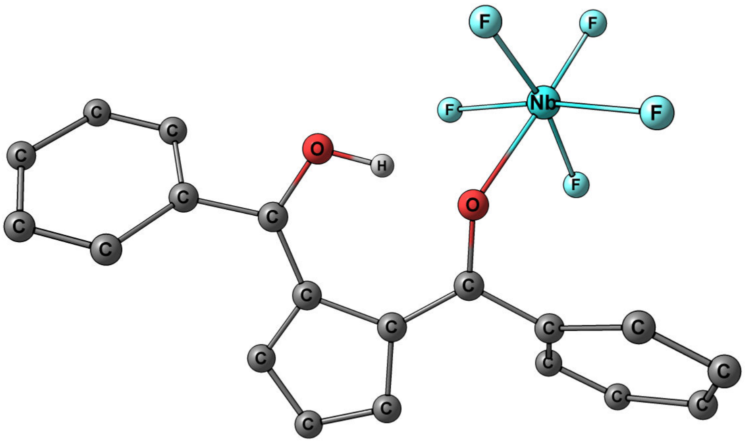

7A

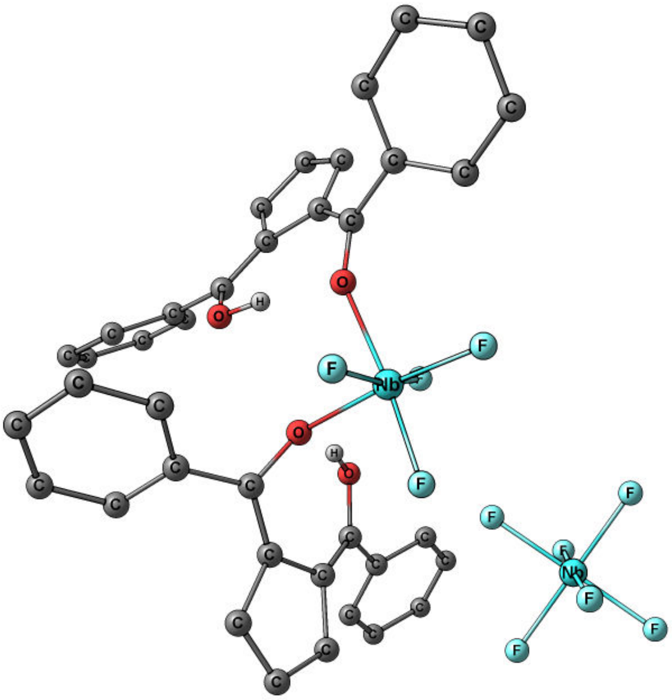

7B

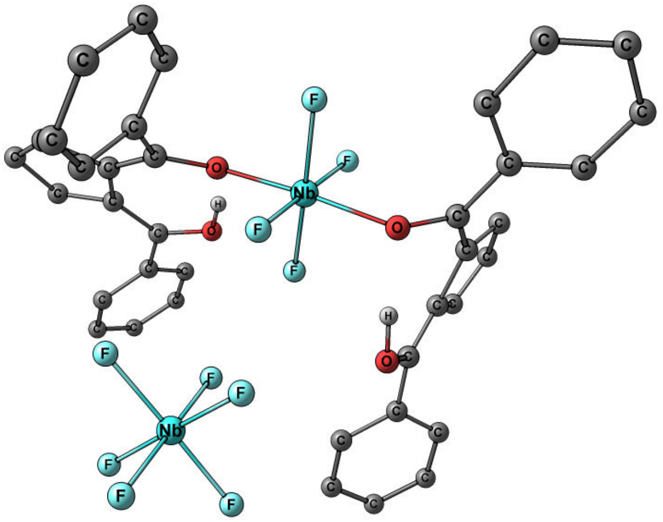

7C

Relative energies (Kcal mol^{-1}, corrected for zero-point vibrational energy, referred to Nb units).

	7A	**7B**	**7C**
PBE/COSMO/DNP	–5.4	0	–2.1

Table S5. Selected computed bond lengths (Å) and angles (°) for **7A** (see Scheme 2 for atom numbering; PBEPBE/COSMO/DNP calculations).

Bond		**Angle**	
Nb–O	2.141	O–Nb–F (*trans* to O)	177.0
Nb–F (*trans* to O)	1.908	O–Nb–F (*cis* to O)	82.2
Nb–F (*cis* to O)	1.923		85.8
	1.919		90.4
	1.918		85.0
	1.929	C–O–Nb	134.7
C–O (coordinated)	1.322	C7–C6–C2	129.8
C–OH	1.320	C1–C2–C3	124.9
C1–C2	1.404	C6–C7–OH	123.5
C2–C3	1.415		
C3–C4	1.393		
C4–C5	1.394		
C5–C6	1.414		
C6–C7	1.401		
O–H	1.027		
(O)H···F (*shortest*)	2.559		
(O)H···O	1.525		

Figure S7. ^{13}C NMR spectrum (CD_2Cl_2) of $NbF_5[\kappa^1(O)\text{-}OC_6H_4CH{=}NHC_6H_3(CHMe_2)_2]$, **2**.

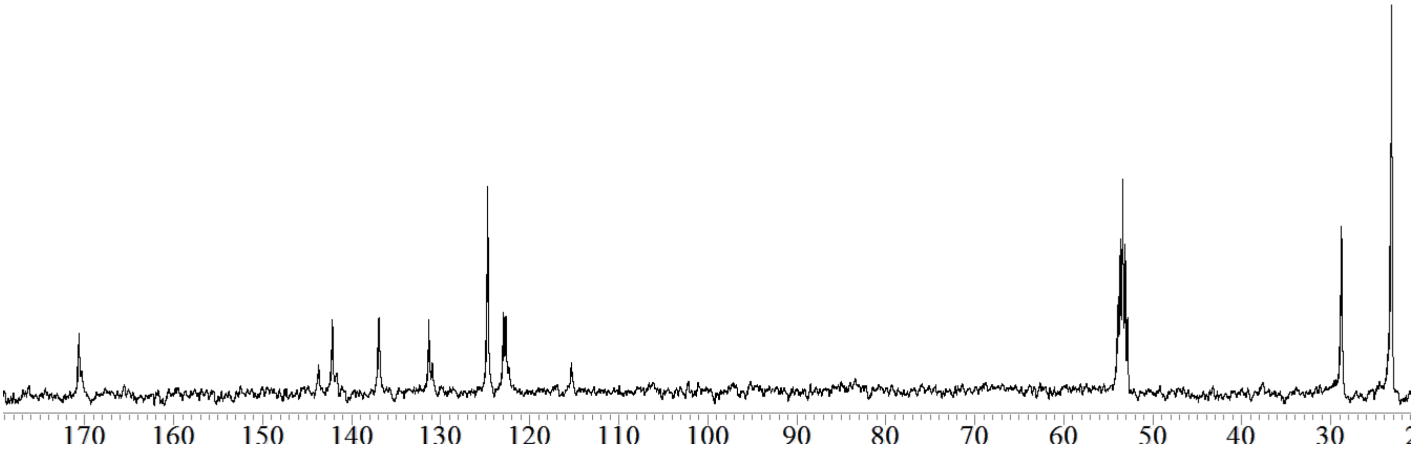

Figure S8. ^{1}H-^{13}C HSQC spectrum (CD_2Cl_2) of $NbF_5[\kappa^1(O)\text{-}OC_6H_4CH{=}NHC_6H_3(CHMe_2)_2]$, **2**.

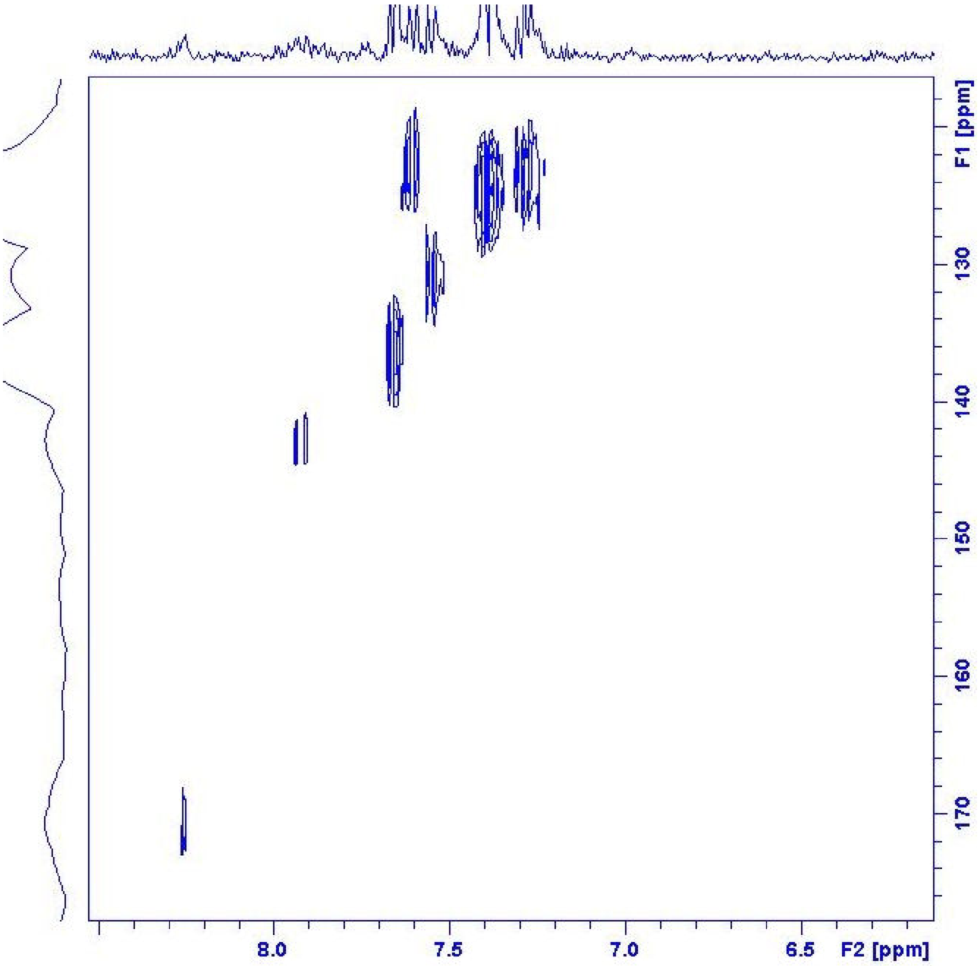

Figure S9. ^{1}H-^{13}C HMBC spectrum (CD_2Cl_2) of $NbF_5[\kappa^1(O)\text{-}OC_6H_4CH{=}NHC_6H_3(CHMe_2)_2]$, **2**.

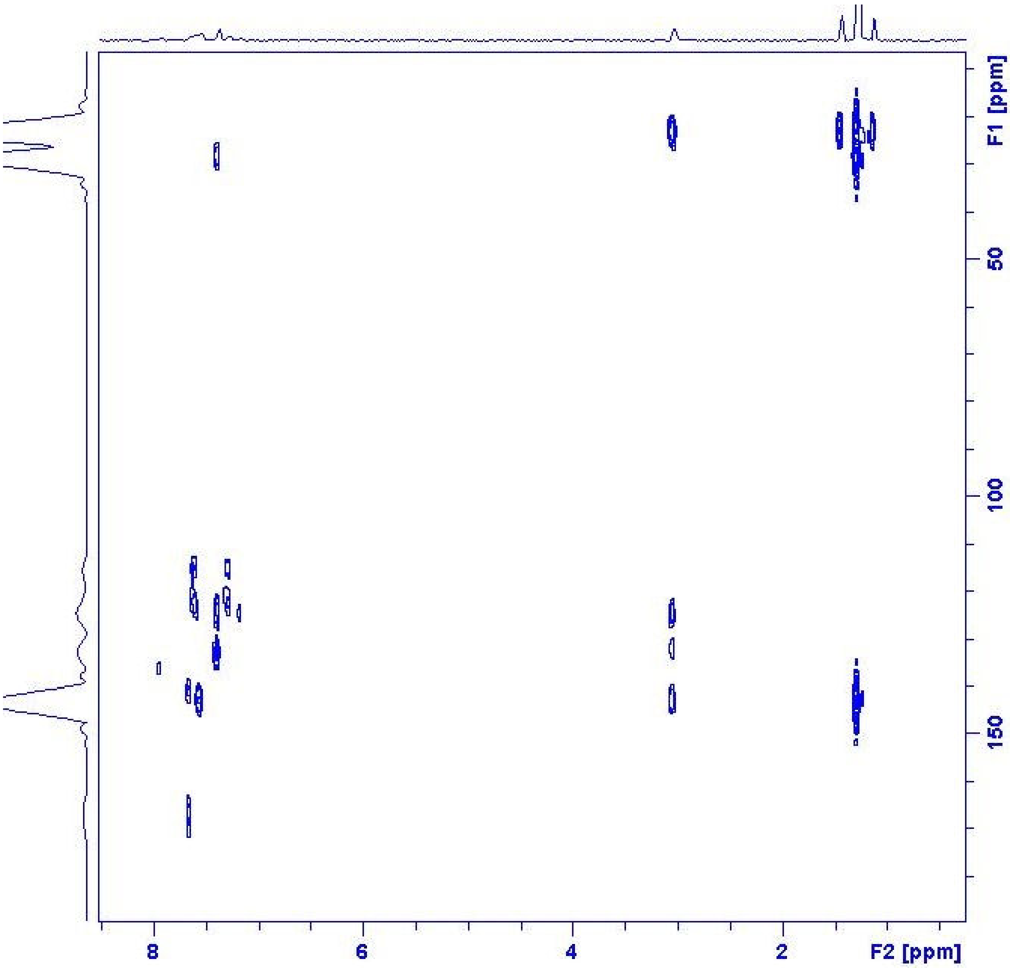

Figure S10. ^{13}C NMR spectrum (CD_2Cl_2) of $[NbCl_2\{\kappa^1(N):\kappa^1(O)\text{-dpimp}\}_2][NbCl_6]$, **4a**.

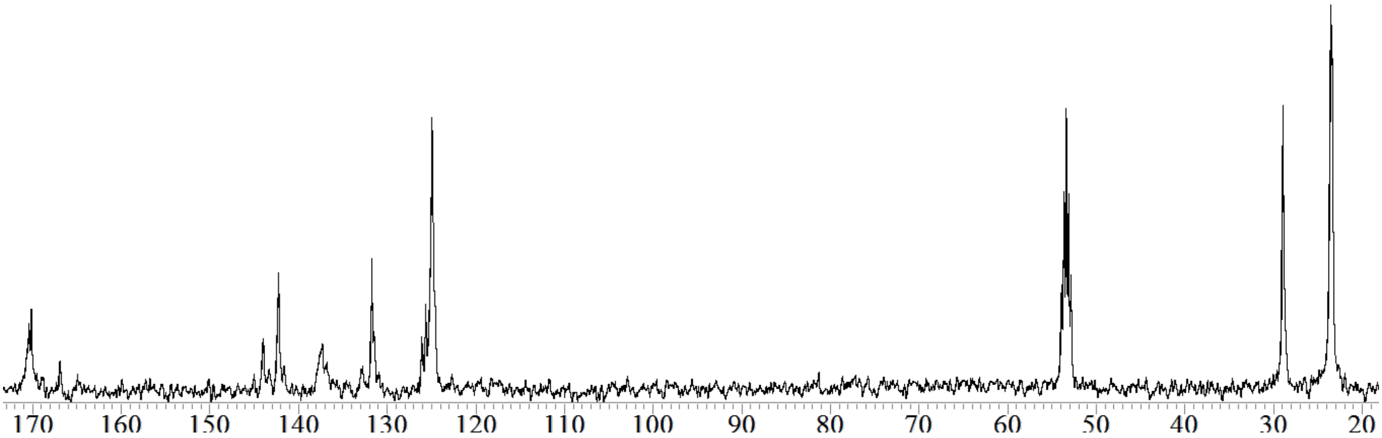

Figure S11. ^{1}H-^{13}C HMBC spectrum (CD_2Cl_2) of $[NbCl_2\{\kappa^1(N):\kappa^1(O)\text{-dpimp}\}_2][NbCl_6]$, **4a**.

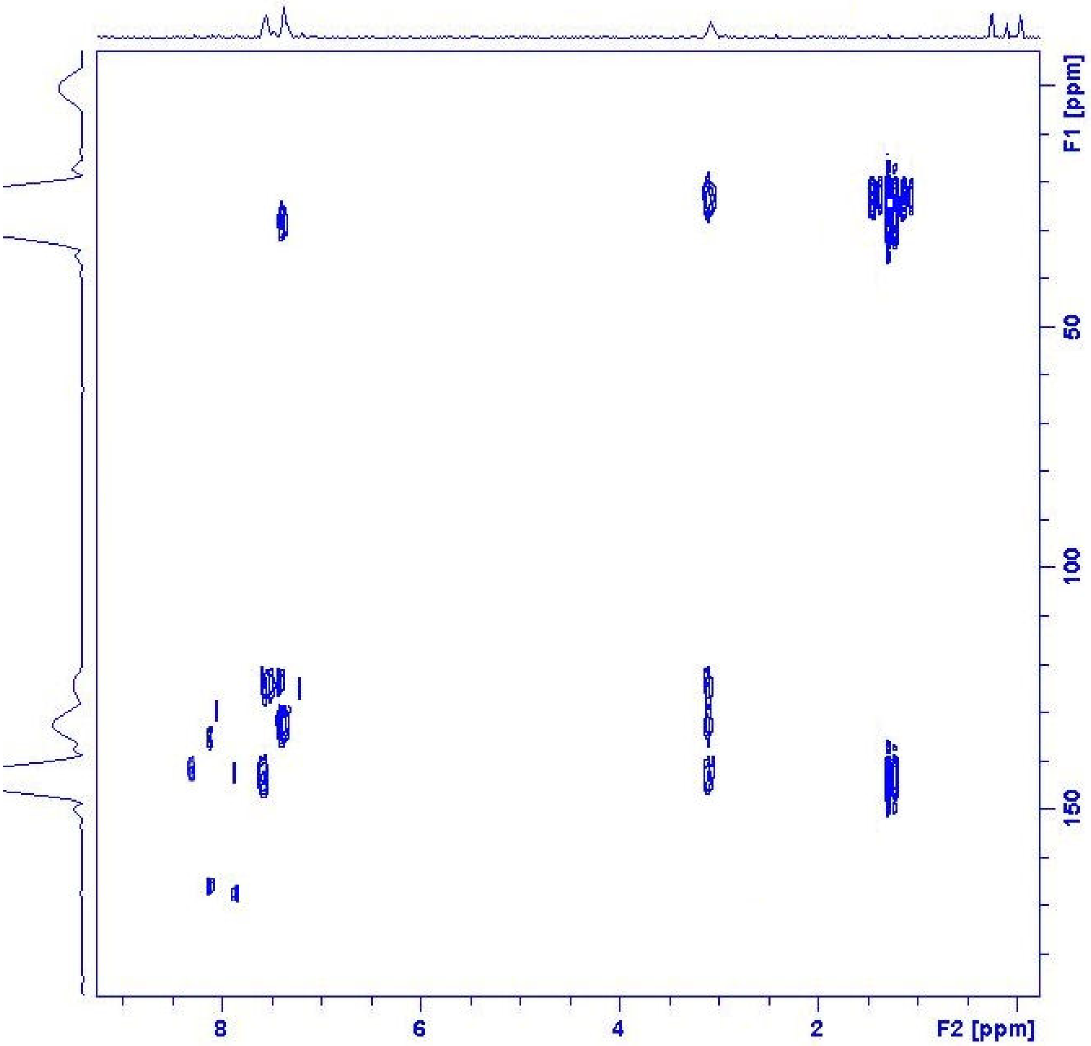

Figure S12. ^{13}C NMR spectrum (CD_2Cl_2) of [$TaCl_2$\{κ^1(*N*):κ^1(*O*)-dpimp\}$_2$][$TaCl_6$], **4b**.

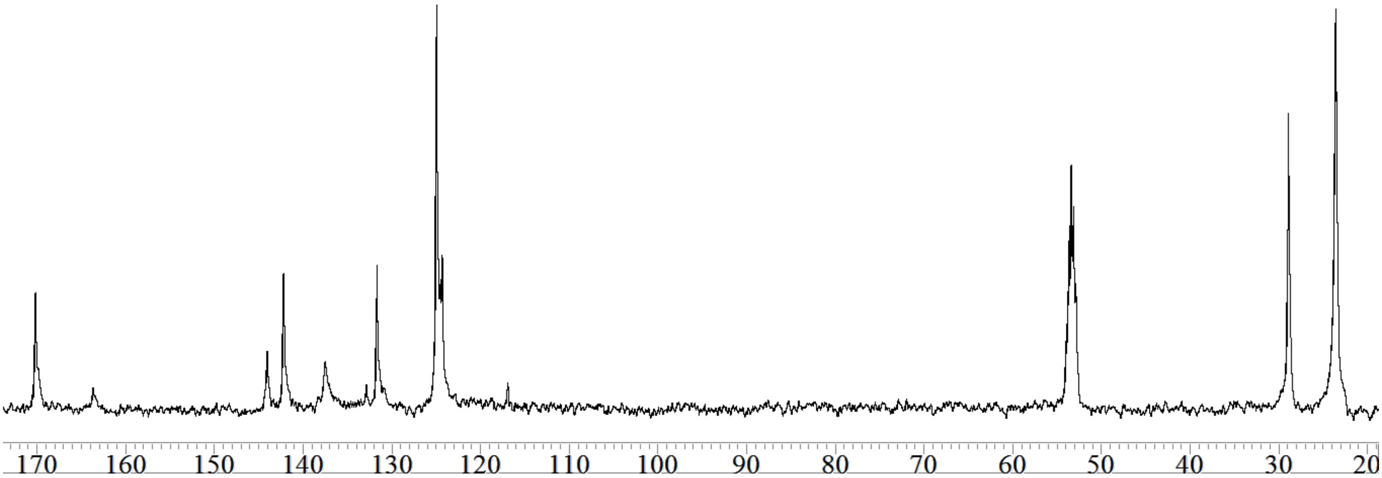

Figure S13. ^{1}H-^{13}C HSQC spectrum (CD_2Cl_2) of [$TaCl_2$\{κ^1(*N*):κ^1(*O*)-dpimp\}$_2$][$TaCl_6$], **4b**.

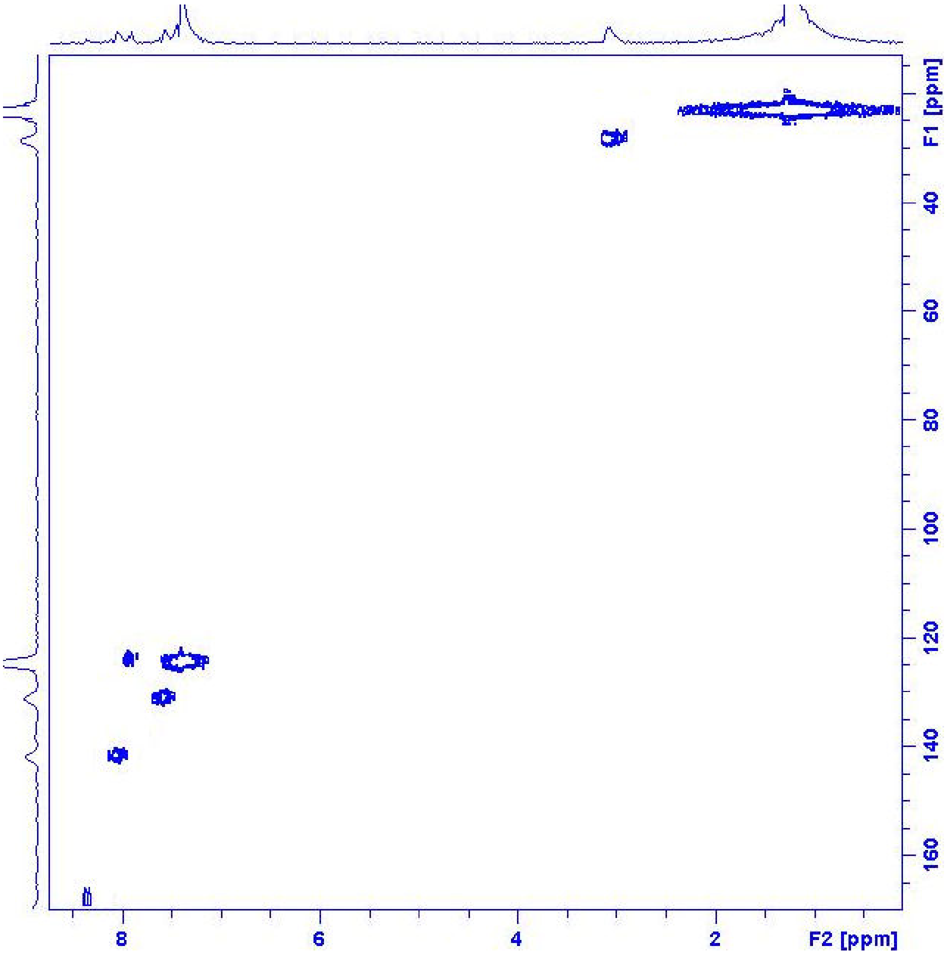

Figure S14. ^{1}H-^{13}C HMBC spectrum (CD_2Cl_2) of [$TaCl_2${κ^1(*N*):κ^1(*O*)-dpimp}$_2$][$TaCl_6$], **4b**.

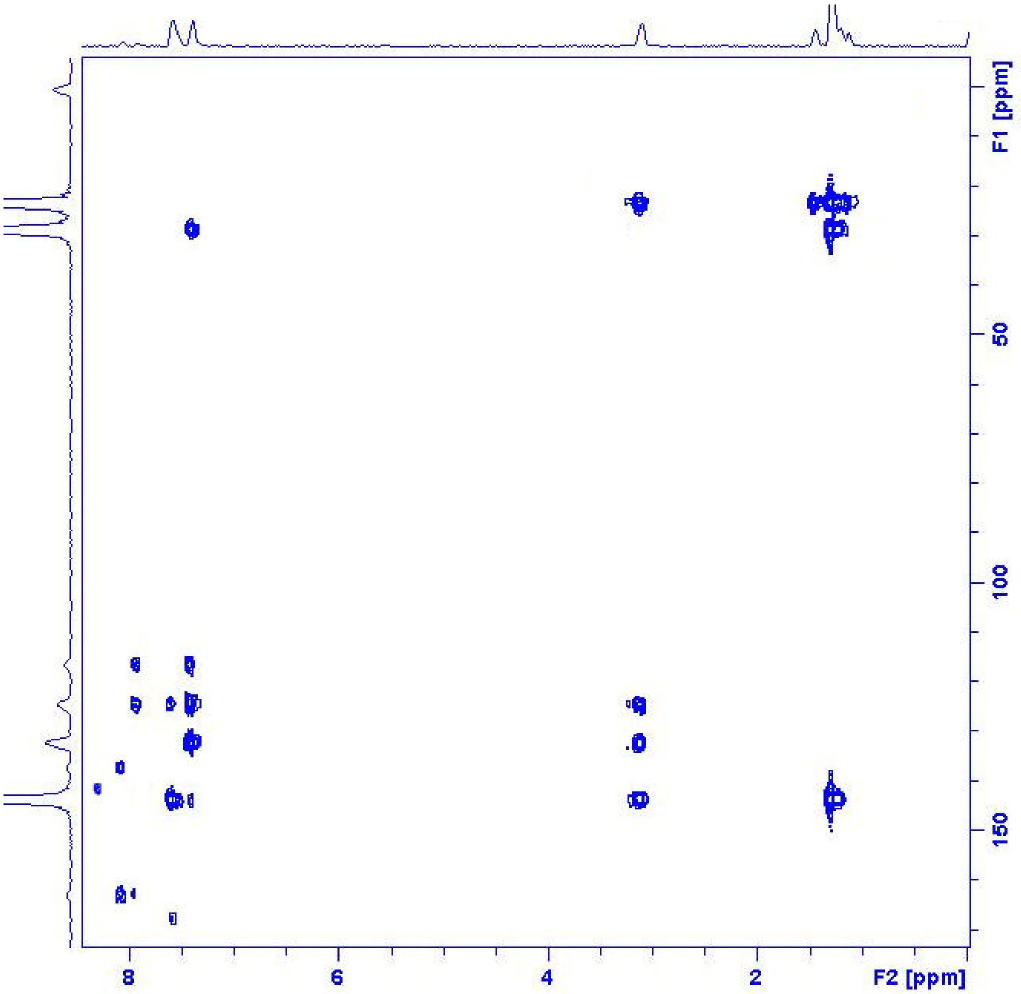

Figure S15. ^{13}C NMR spectrum ($CDCl_3$) of 2-[(2,6-Diisopropylphenyl)iminomethyl]phenol (**dpimpH**).

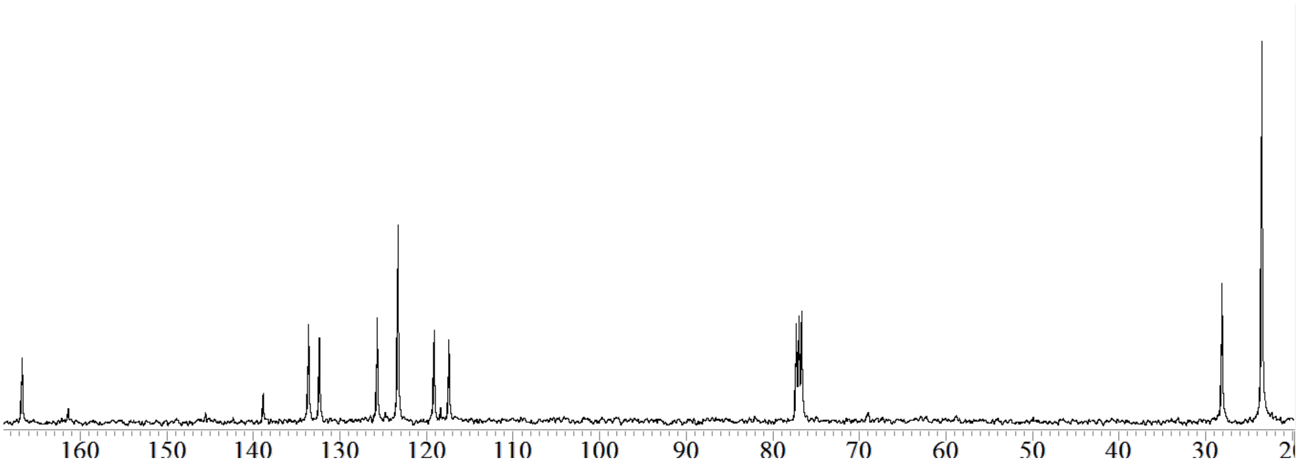

Figure S16. ^{1}H-^{13}C HSQC spectrum ($CDCl_3$) of 2-[(2,6-Diisopropylphenyl)iminomethyl]phenol (**dpimpH**).

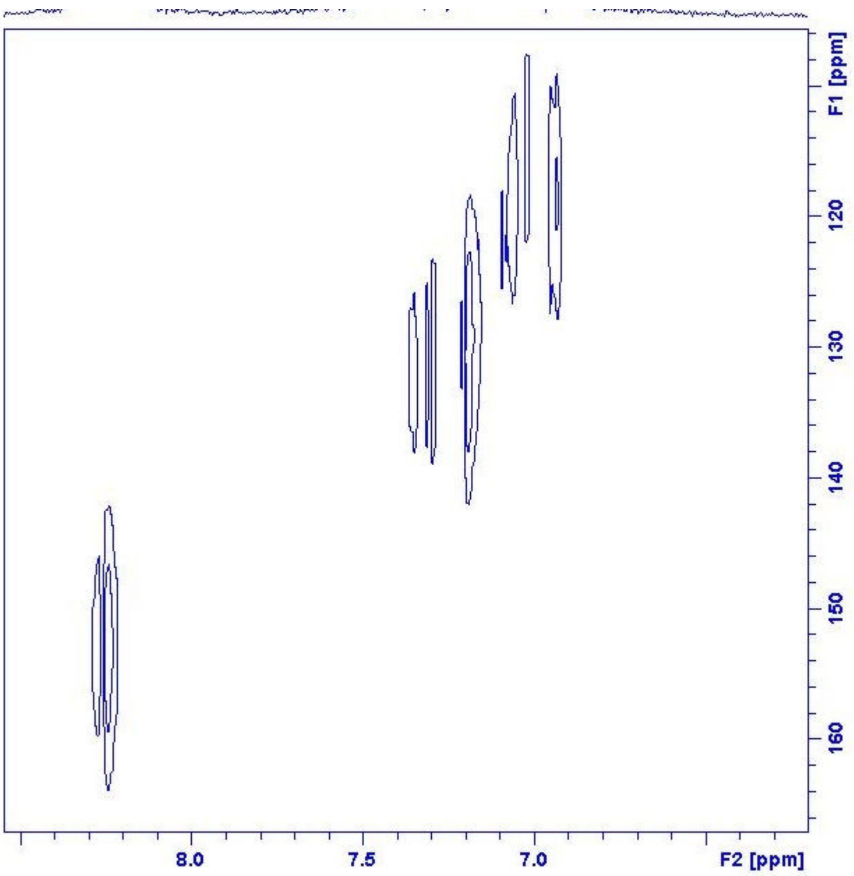

Figure S17. ^{1}H-^{13}C HMBC spectrum ($CDCl_3$) of 2-[(2,6-Diisopropylphenyl)iminomethyl]phenol (**dpimpH**).

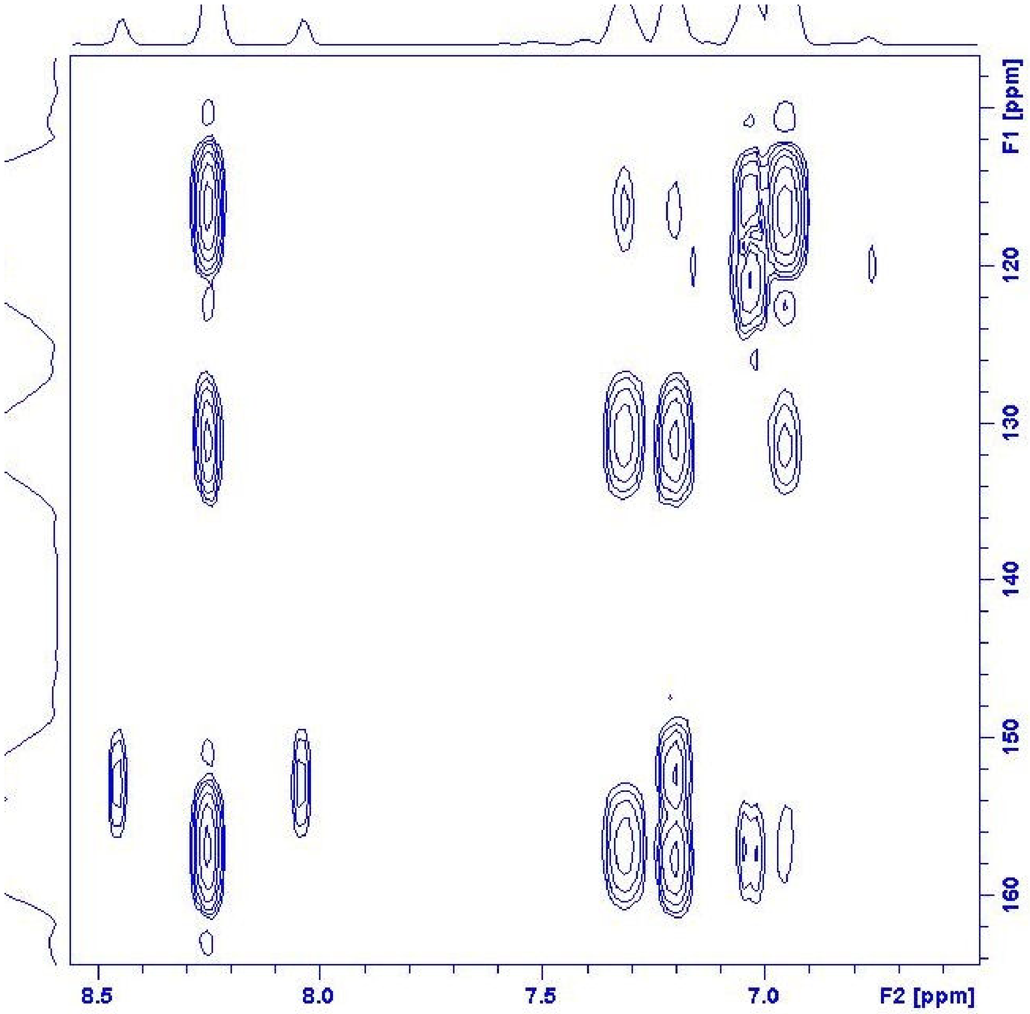

Figure S18. ^{13}C NMR spectrum (CD$_3$CN) of [NbF$_4${κ^1(*O*)-ON(H)=CHC$_6$H$_4$OH}$_2$][NbF$_6$], **3**.

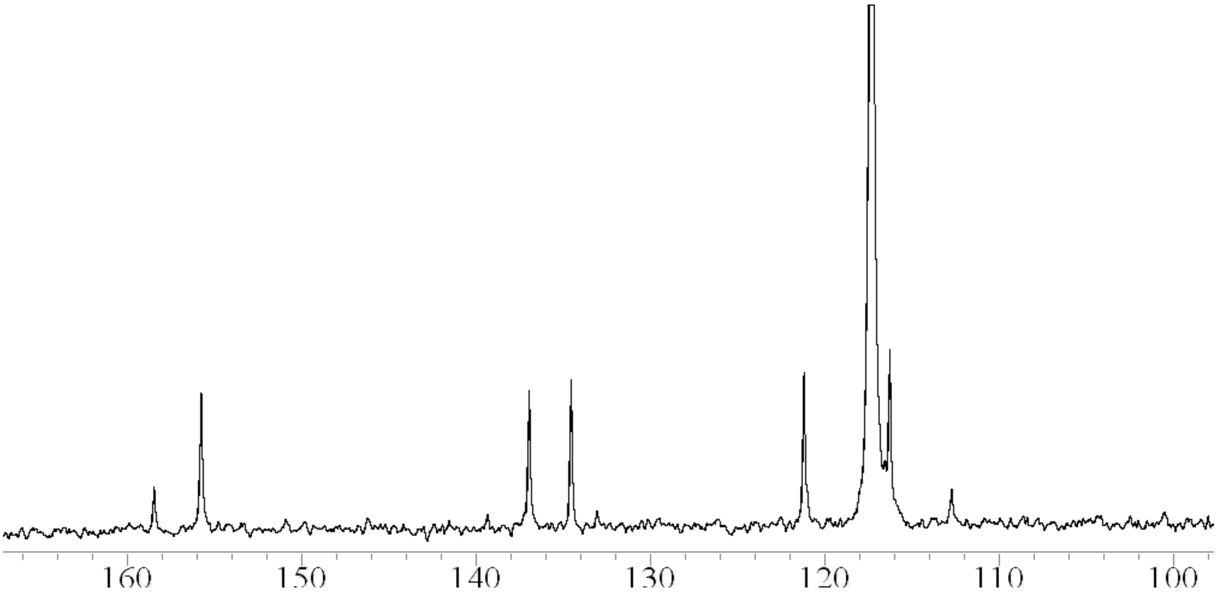

Figure S19. ^{1}H-^{13}C HSQC spectrum (CD$_3$CN) of [NbF$_4${κ^1(*O*)-ON(H)=CHC$_6$H$_4$OH}$_2$][NbF$_6$], **3**.

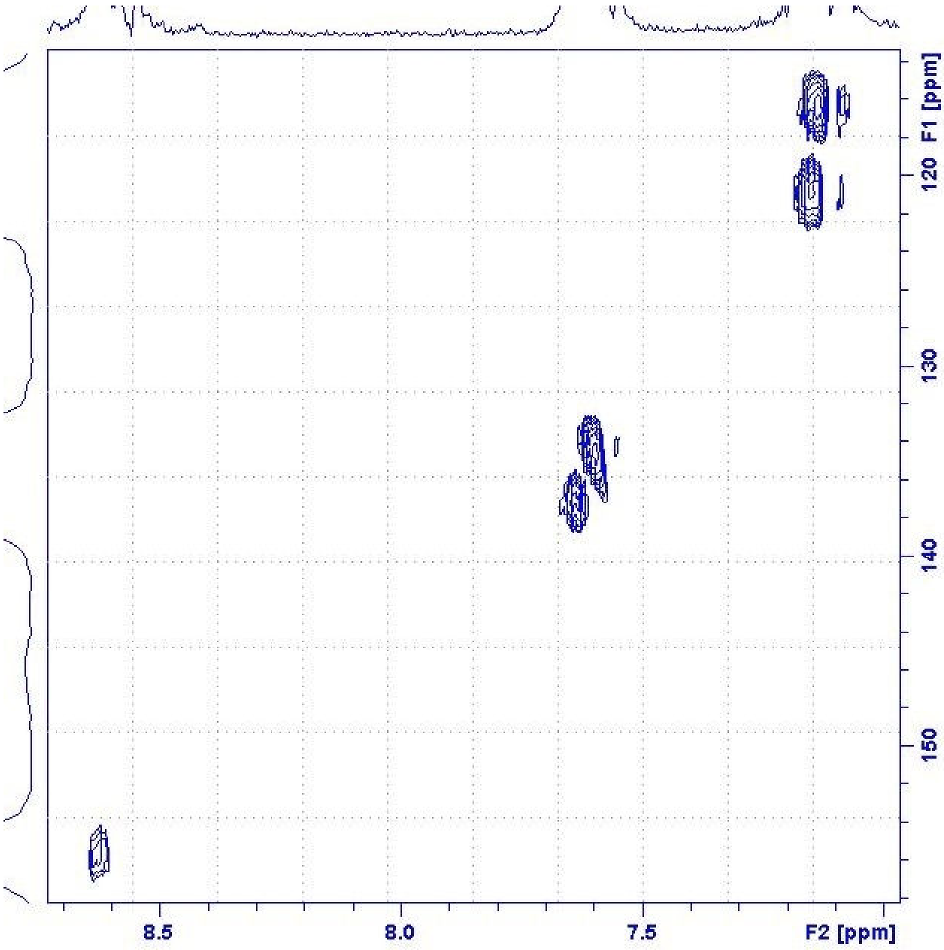

Figure S20. ^{1}H-^{13}C HMBC spectrum (CD$_3$CN) of [NbF$_4${κ^1(*O*)-ON(H)=CHC$_6$H$_4$OH}$_2$][NbF$_6$], **3**.

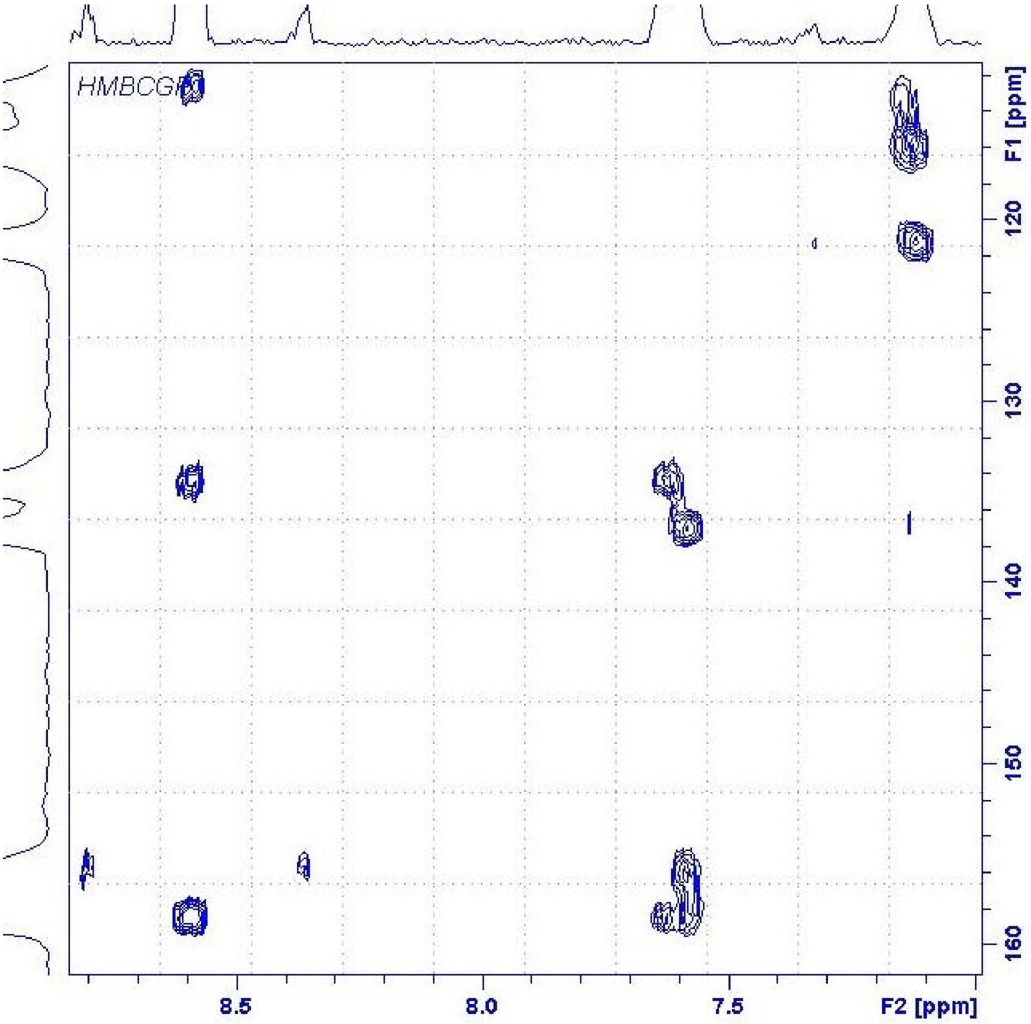

Figure S21. ^{13}C NMR spectrum (CD_2Cl_2) of Nb_2Cl_7[κ^1(*O*)-saoH][κ^2(*O*)-sao], **5**.

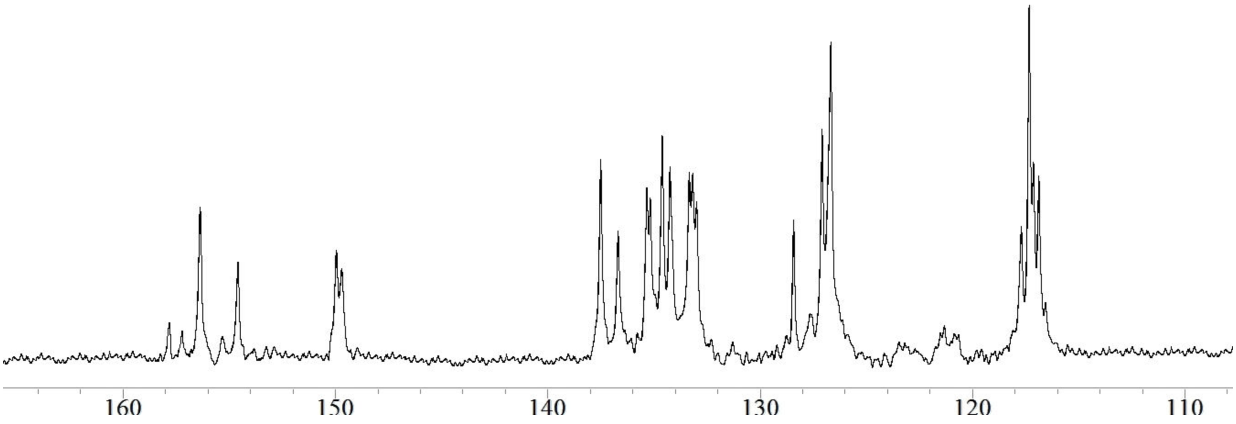

Figure S22. ^{1}H-^{13}C HSQC spectrum (CD_2Cl_2) of Nb_2Cl_7[κ^1(*O*)-saoH][κ^2(*O*)-sao], **5**.

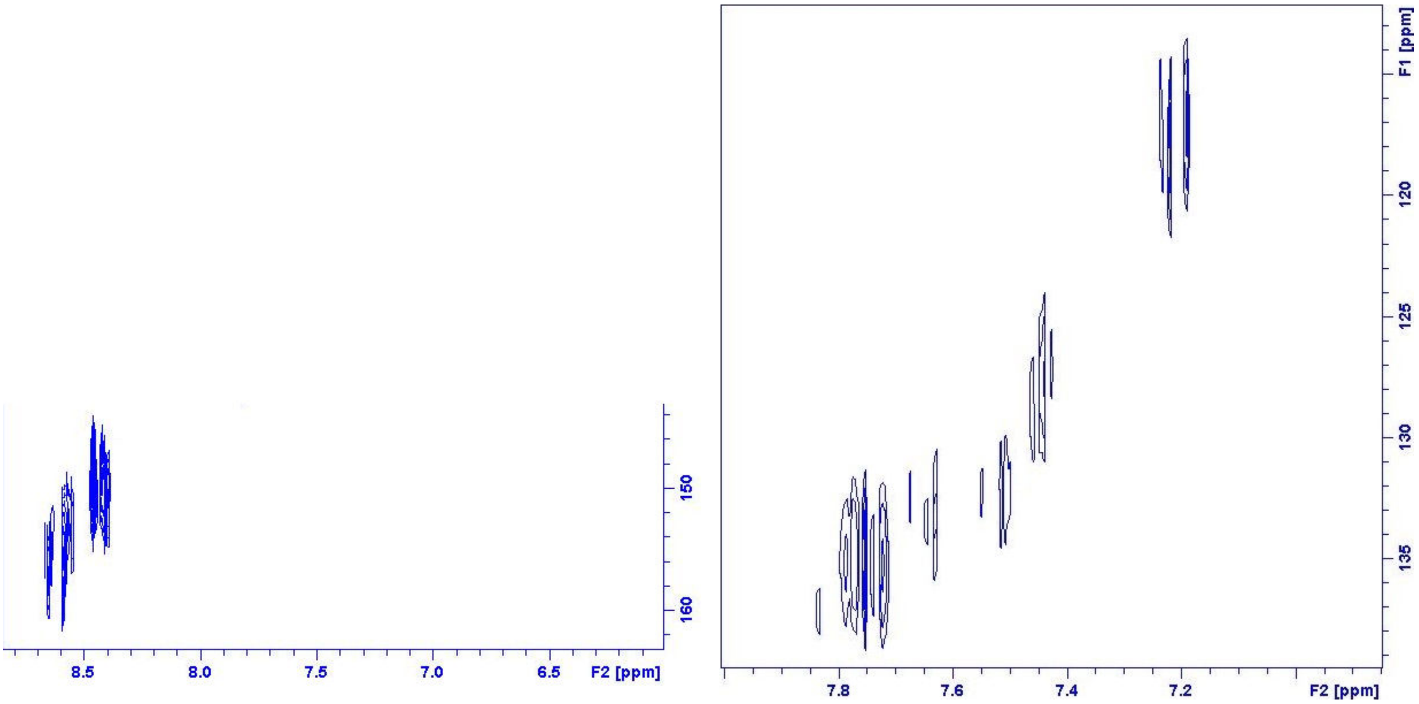

Figure S23. ^{1}H-^{13}C HMBC spectrum (CD_2Cl_2) of $Nb_2Cl_7[\kappa^1(O)\text{-saoH}][\kappa^2(O)\text{-sao}]$, **5**.

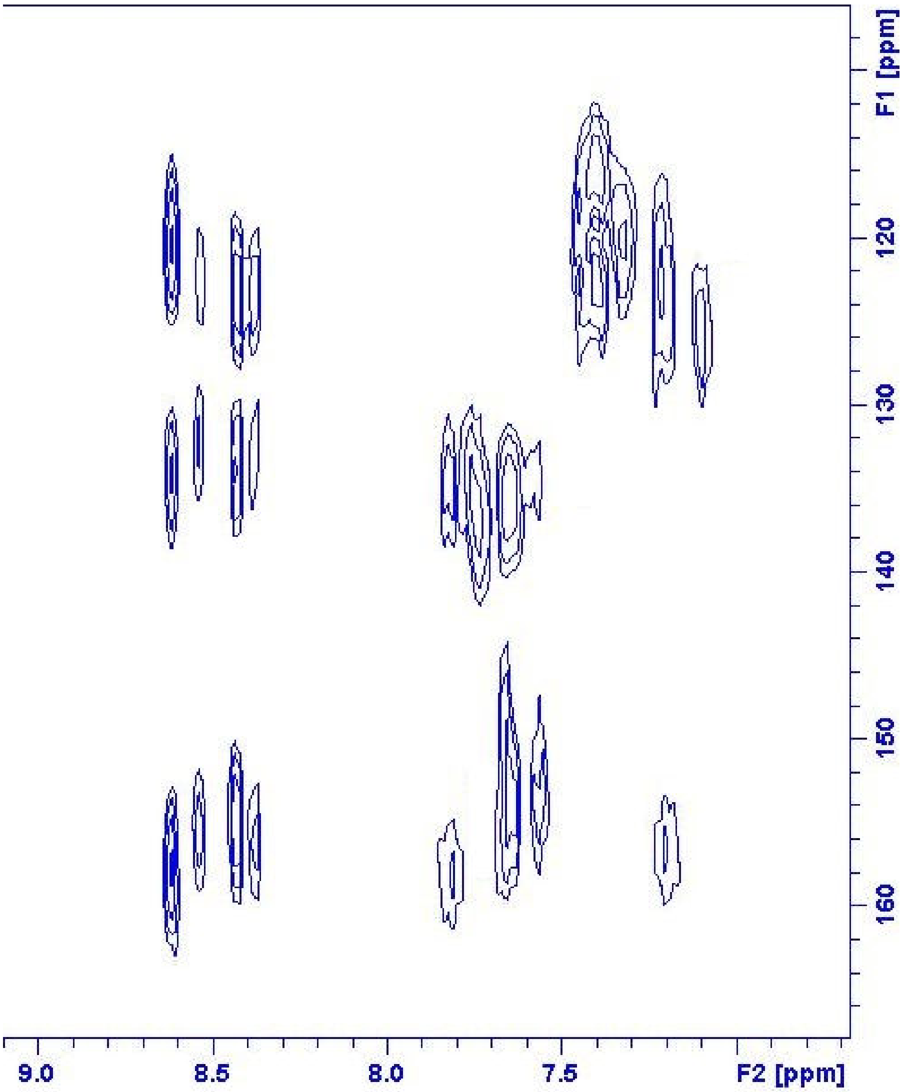

Figure S24. ^{13}C NMR spectrum ($CDCl_3$) of salicylaldehyde oxime (**saoH$_2$**).

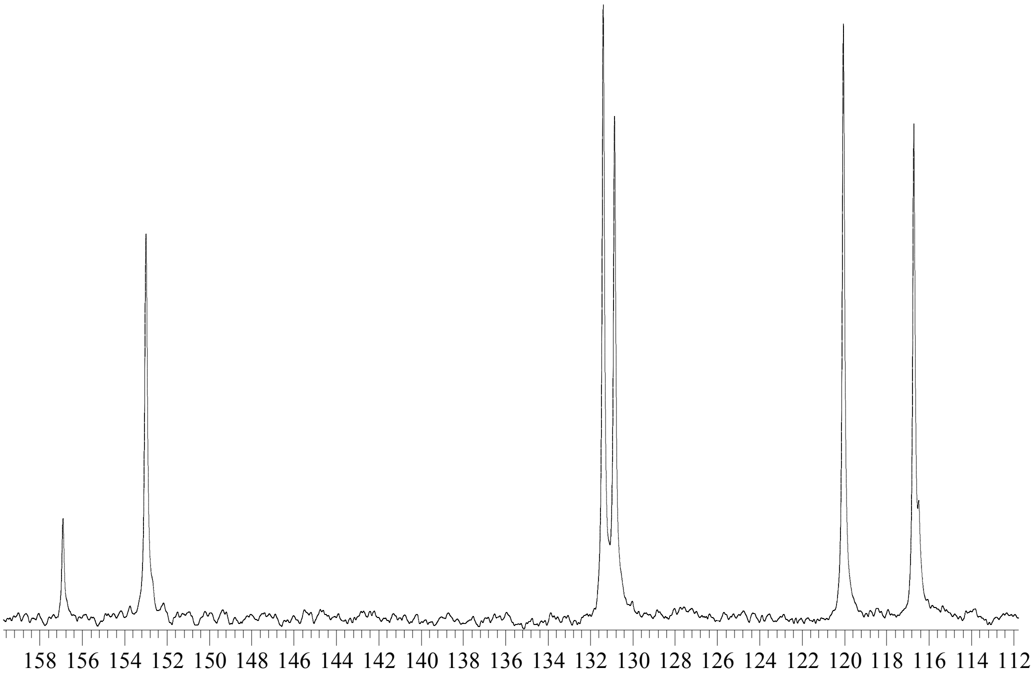

Figure S25. ^{1}H-^{13}C HSQC spectrum of salicylaldehyde oxime (**saoH$_2$**).

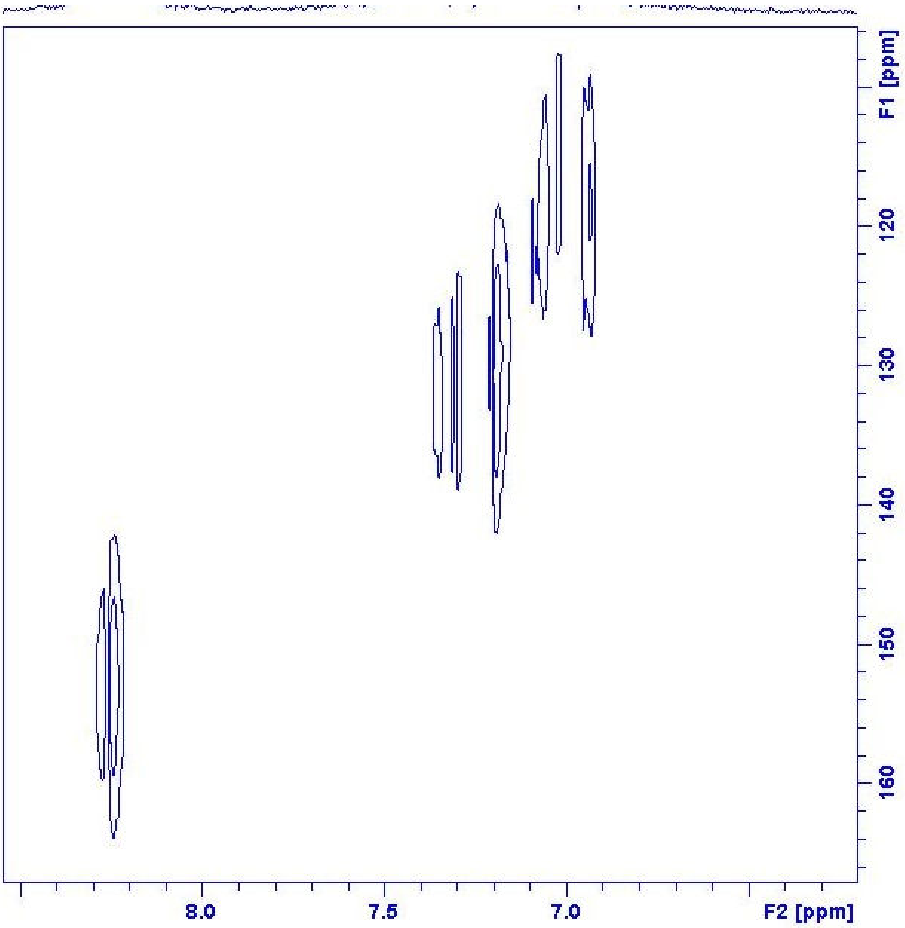

Figure S26. ^{1}H-^{13}C HMBC spectrum ($CDCl_3$) of salicylaldehyde oxime (**saoH$_2$**).

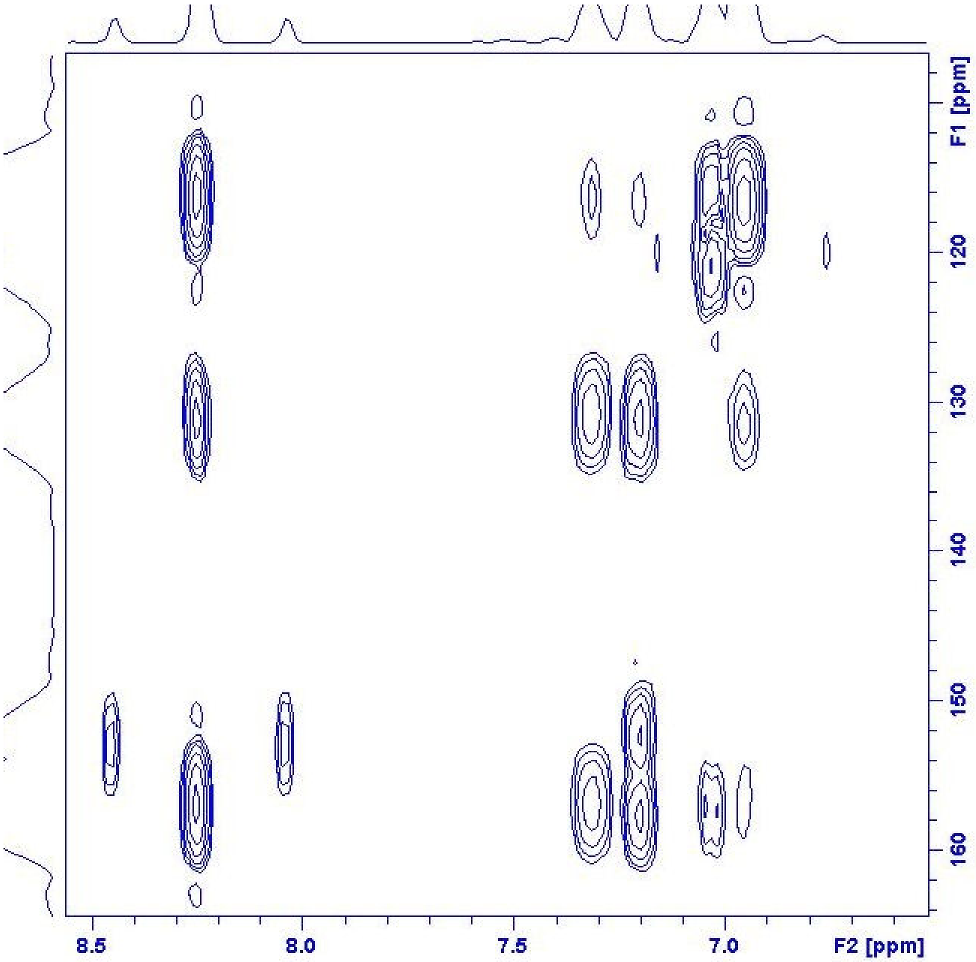

Figure S27. ^{13}C NMR spectrum (CD_2Cl_2) of $NbF_5[\kappa^1(O)\text{-bhpfH}]$, **7**.

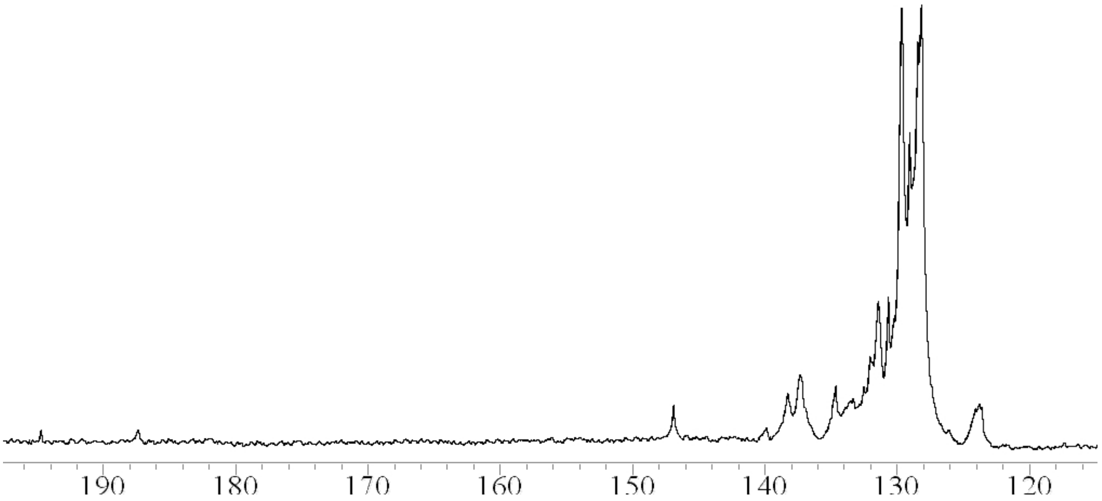

Figure S28. ^{1}H-^{13}C HSQC spectrum (CD_2Cl_2) of $NbF_5[\kappa^1(O)\text{-bhpfH}]$, **7**.

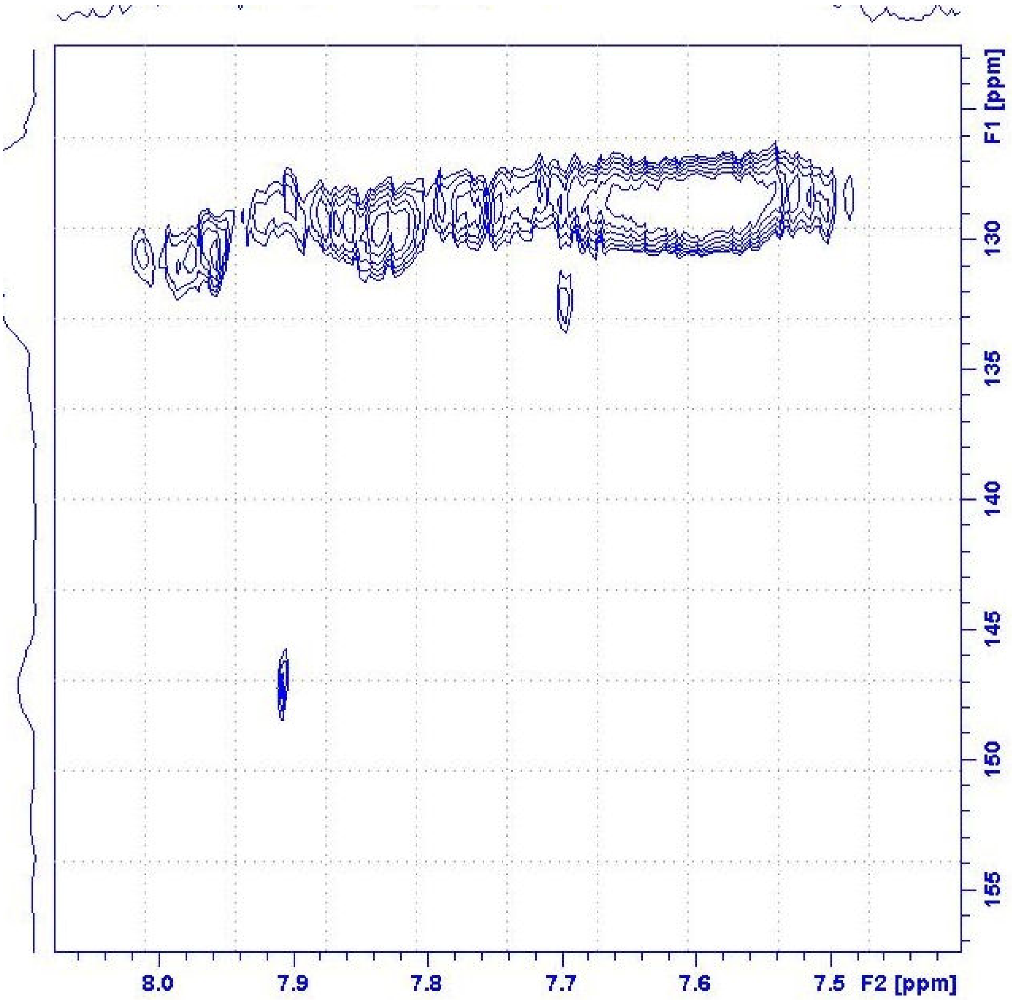

Figure S29. ^{1}H-^{13}C HMBC spectrum (CD_2Cl_2) of $NbF_5[\kappa^1(O)\text{-bhpfH}]$, **7**.

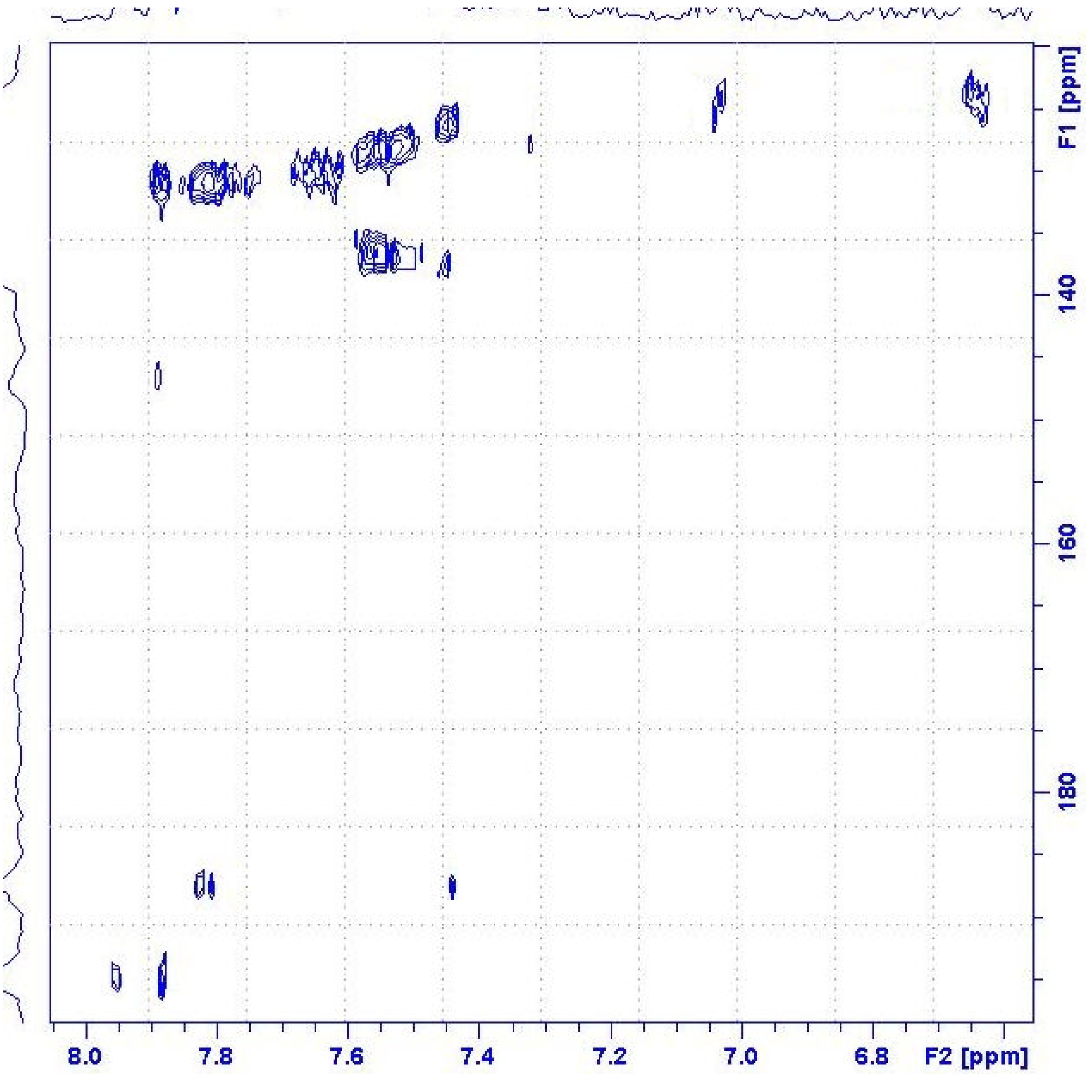

Figure S30. ^{13}C NMR spectrum (CD_2Cl_2) of $NbCl_4[\kappa^2(O)$-bhpf], **8**.

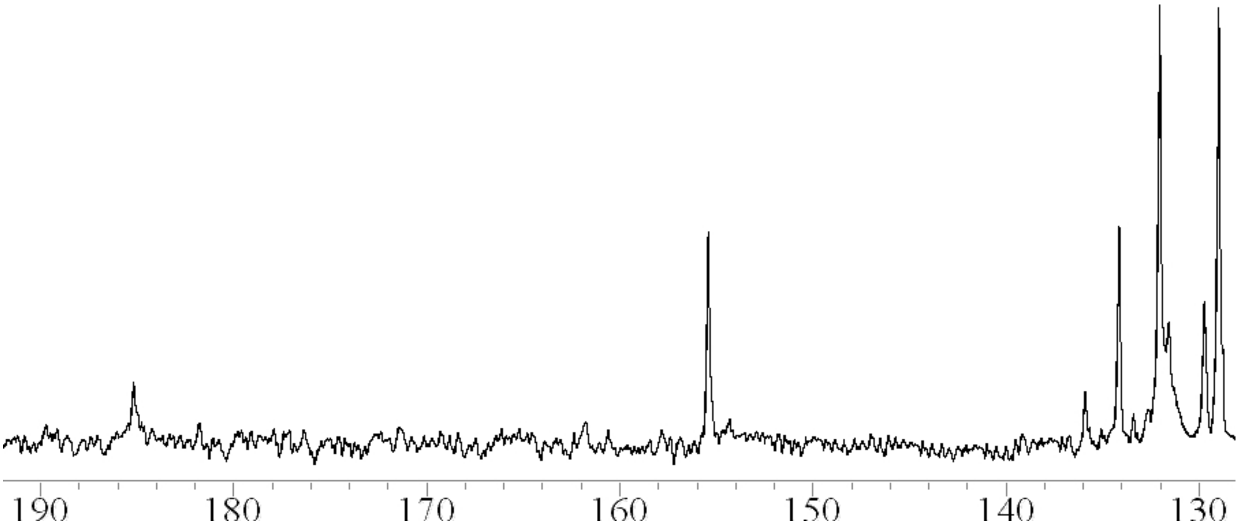

Figure S31. ^{1}H-^{13}C HSQC spectrum (CD_2Cl_2) of $NbCl_4[\kappa^2(O)$-bhpf], **8**.

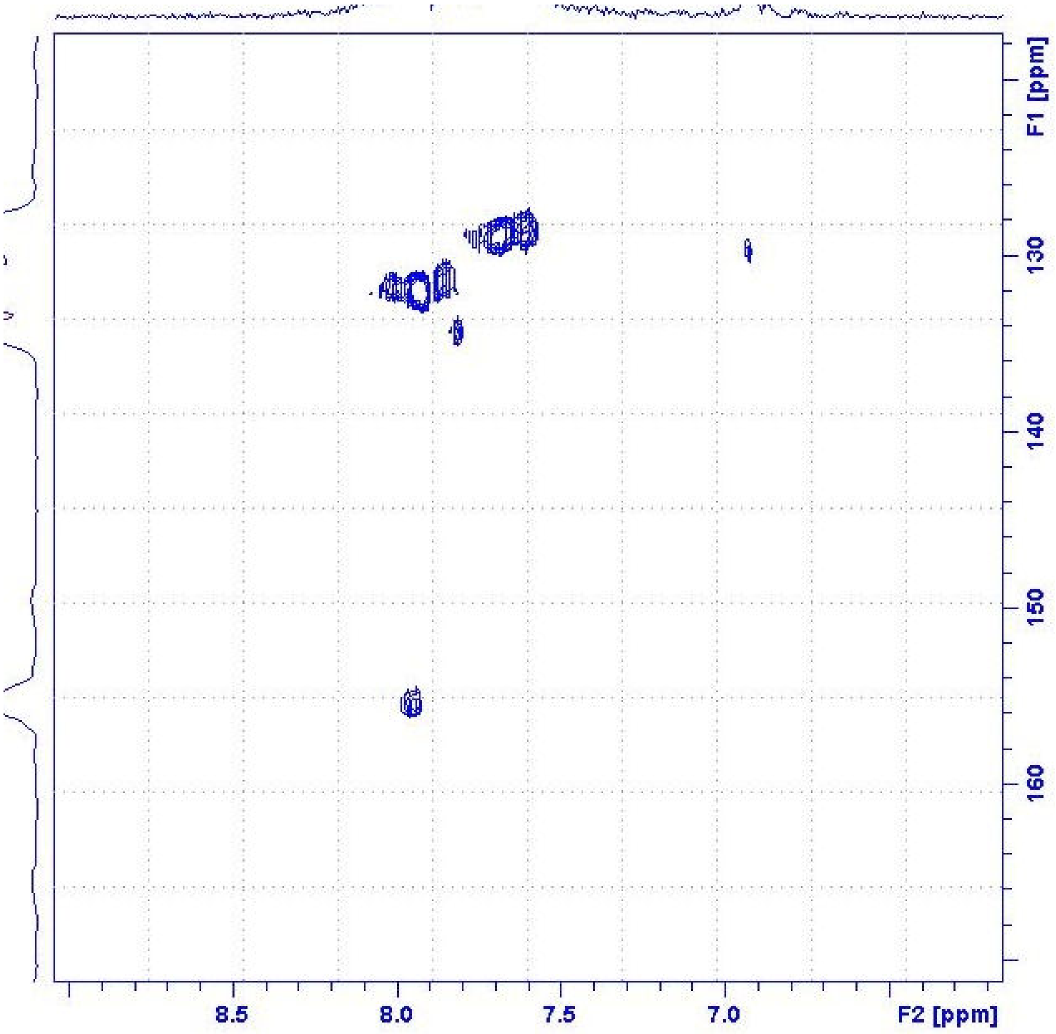

Figure S32. ^{1}H-^{13}C HMBC spectrum (CD_2Cl_2) of $NbCl_4[\kappa^2(\textit{O})\text{-bhpf}]$, **8**.

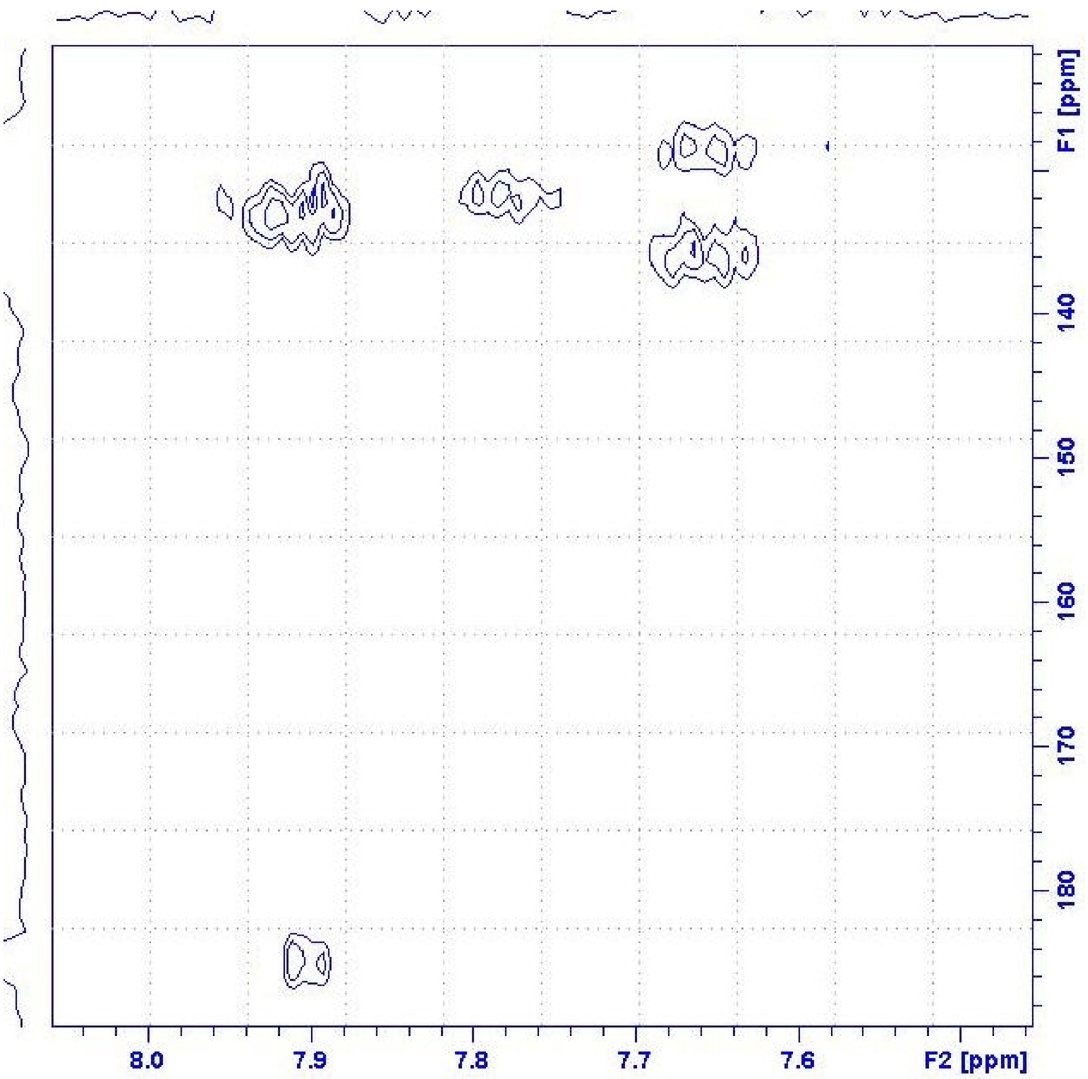

Figure S33. ^{13}C NMR spectrum ($CDCl_3$) of 2-Benzoyl-6-hydroxy-6-phenylpentafulvene (**bhpfH**).

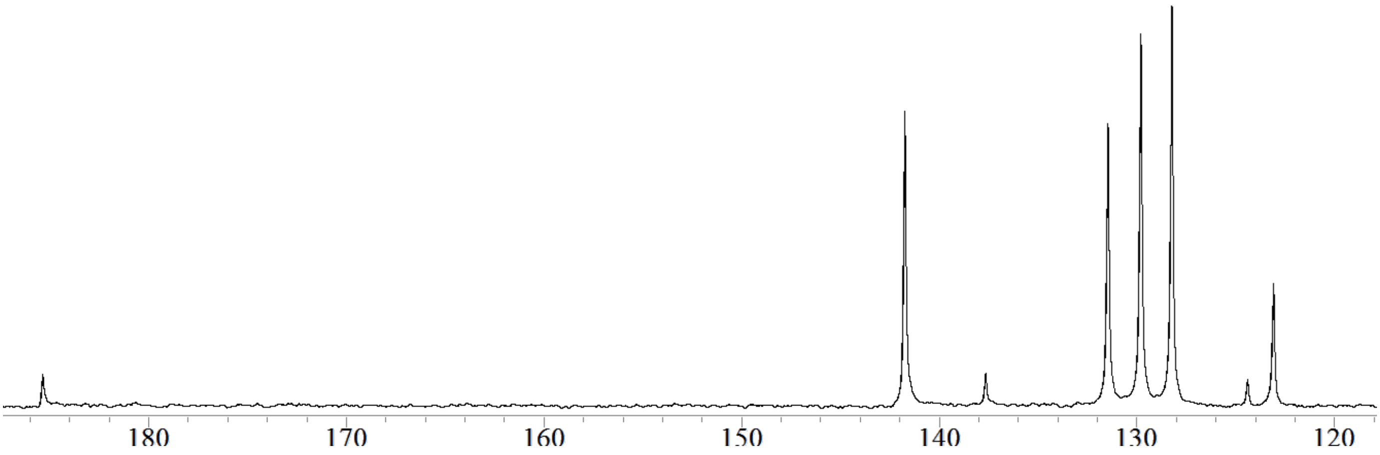

Figure S34. ^{1}H-^{13}C HSQC spectrum ($CDCl_3$) of 2-Benzoyl-6-hydroxy-6-phenylpentafulvene (**bhpfH**).

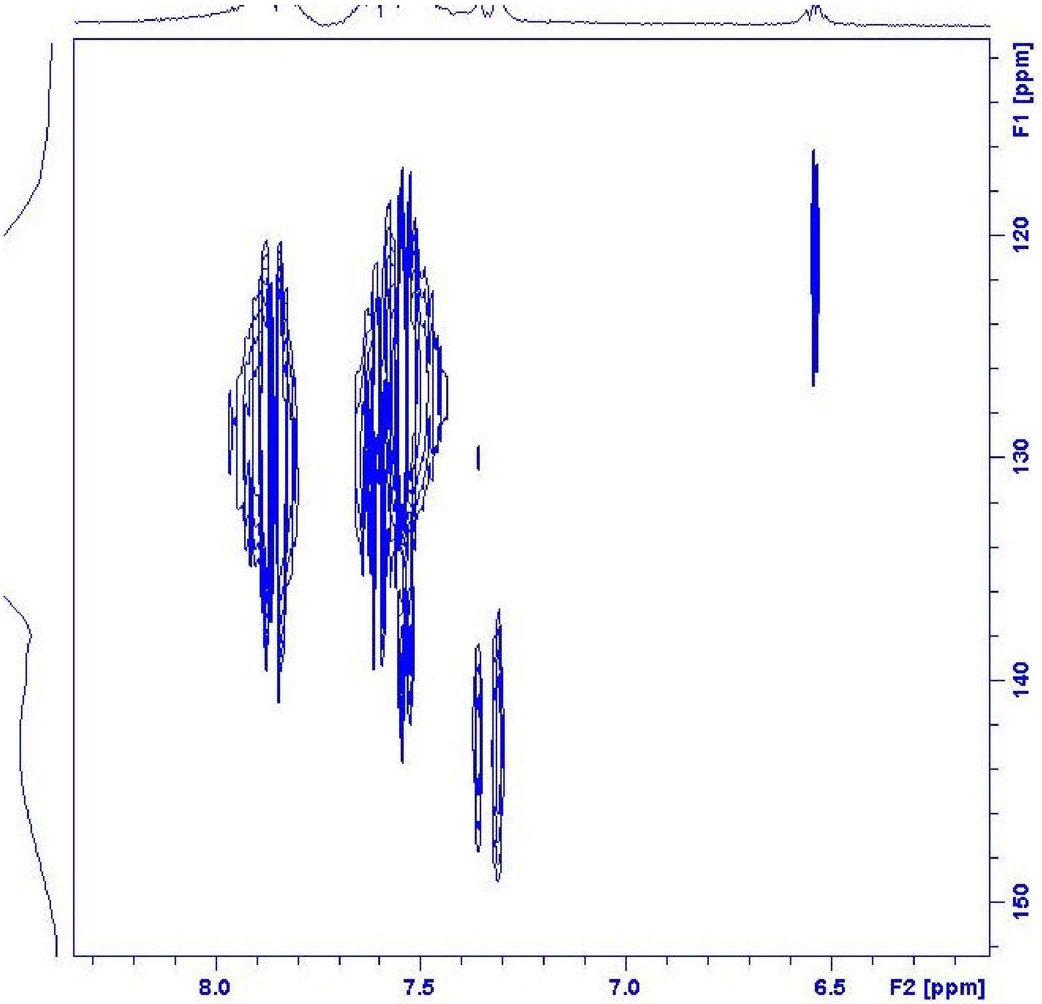

Figure S35. ^{1}H-^{13}C HMBC spectrum (CDCl$_3$) of 2-Benzoyl-6-hydroxy-6-phenylpentafulvene (**bhpfH**).